AD-A046 729 BLOCK ENGINEERING INC CAMBRIDGE MASS F/G 19/1
AN NQR STUDY OF TNT CHARACTERISTICS.(U)
SEP 77 R A MARINO, D WADE, S M KLAINER DAAG29-76-C-0025
UNCLASSIFIED BEI-77-701 ARO-13768.1-PX NL

END
DATE FILMED
12-77
DDC

AD A046729

12

BLOCK
ENGINEERING, INC.

Cambridge, Mass. 02139 •

(12)

(14) BEI-77-701

(6) AN NQR STUDY OF TNT CHARACTERISTICS.

(9) FINAL TECHNICAL REPORT. 22 Mar 76-31 Aug 77

(11) September 1977 (12) 68 p.

by

(10) Robert A. Marino,
Donald Wade
Stanley M. Klainer

Submitted to

Department of the Army
U.S. Army Research Office
Research Triangle Park
North Carolina 27709

(18) ARO

(19) 13768.1-PX

Contract No. DAAG-29-76-C-0025

(15)

Submitted by

BLOCK ENGINEERING, INC.
19 Blackstone Street
Cambridge, Massachusetts 02139

059 070

SECURITY CLASSIFICATION OF THIS PAGE (When Data Entered)

ARO 13768.1-PX

REPORT DOCUMENTATION PAGE

READ INSTRUCTIONS BEFORE COMPLETING FORM

1. REPORT NUMBER: 13768.1-PX	2. GOVT ACCESSION NO.
3. RECIPIENT'S CATALOG NUMBER	
4. TITLE (and Subtitle): An NQR Study of TNT Characteristics	5. TYPE OF REPORT & PERIOD COVERED: Final Report: 22 Mar 76 - 31 Aug 77
6. PERFORMING ORG. REPORT NUMBER	
7. AUTHOR(s): Robert A. Marino, Donald Wade, Stanley M. Klainer	8. CONTRACT OR GRANT NUMBER(s): DAAG29 76 C 0025
9. PERFORMING ORGANIZATION NAME AND ADDRESS: Block Engineering, Inc., 19 Blackstone Street, Cambridge, Massachusetts 02139	10. PROGRAM ELEMENT, PROJECT, TASK AREA & WORK UNIT NUMBERS
11. CONTROLLING OFFICE NAME AND ADDRESS: U. S. Army Research Office, Post Office Box 12211, Research Triangle Park, NC 27709	12. REPORT DATE: Sep 77 13. NUMBER OF PAGES: 65
14. MONITORING AGENCY NAME & ADDRESS (if different from Controlling Office)	15. SECURITY CLASS. (of this report): Unclassified 15a. DECLASSIFICATION/DOWNGRADING SCHEDULE

16. DISTRIBUTION STATEMENT (of this Report)

Approved for public release; distribution unlimited.

17. DISTRIBUTION STATEMENT (of the abstract entered in Block 20, if different from Report)

18. SUPPLEMENTARY NOTES

The findings in this report are not to be construed as an official Department of the Army position, unless so designated by other authorized documents.

19. KEY WORDS (Continue on reverse side if necessary and identify by block number)

TNT	Chemical properties
Explosives	Crystalline states
Spectrometry	Morphology
Nuclear quadrupole resonance	Phase transformations

20. ABSTRACT (Continue on reverse side if necessary and identify by block number) The results of this research have established that the nuclear quadrupole resonance (NQR) spectrometric technique is ideally suited for the characterization of explosives such as TNT. NQR data yields information on chemical structure, crystalline states and morphology. For the explosive TNT it has been shown that: a. TNT exists in two morphological states, b. TNT undergoes a phase transition at approximately 200K. In addition a new mechanism was discovered for obtaining NQR signals at high data rates thus enhancing system efficiency by a factor of up to 100. Finally, initial research was performed using soft ferrite cores in place of the standard sample coils in an effort to reduce the amount of sample required for an NQR measurement.

DD FORM 1 JAN 73 1473 EDITION OF 1 NOV 65 IS OBSOLETE

Unclassified

SECURITY CLASSIFICATION OF THIS PAGE (When Data Entered)

TABLE OF CONTENTS

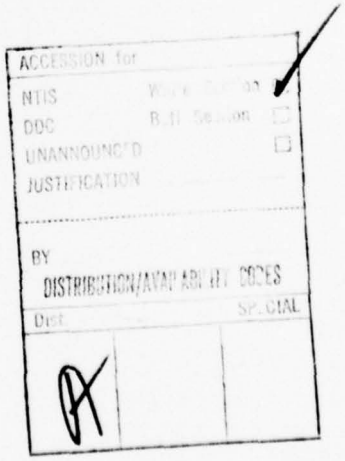

1. INTRODUCTION

1.1 PURPOSE OF PROGRAM

The program described in this report was designed to study the characteristics of TNT using the technique of NQR (nuclear quadrupole resonance) spectroscopy. Emphasis was placed on measuring the polymorphism in TNT between 77°K and room temperature and determining whether any phase changes occur over the same temperature interval. The program approached these measurements from both the theoretical and experimental aspects with emphasis being placed on the laboratory measurements.

1.2 SUMMARY OF PROGRAM RESULTS

The results of this research have established that the NQR spectrometric technique is ideally suited for the characterization of explosives such as TNT. NQR data yields information on chemical structure, crystalline states and morphology. For the explosive TNT it has been shown that:

a. TNT exists in two morphological states

b. TNT undergoes a phase transition at $\sim$200°K

In addition a new mechanism was discovered for obtaining NQR signals at high data rates thus enhancing system efficiency by a factor of up to 100. Finally, initial research was performed using soft ferrite cores in place of the standard sample coils in an effort to reduce the amount of sample required for an NQR measurement.

1.3 PROGRAM BACKGROUND

Substances such as TNT, RDX, HMX, and some of the heavy metal azides have for many years been used as military explosives. The physical and chemical properties of these substances have been the subject of many studies in an effort to establish criteria by which the behavior of these compounds could be reliably predicted. This has led to investigation into the manufacturing, handling, and overall effectiveness of these materials for both military and industrial use.

In spite of these efforts many fundamental questions remain. In fact as a deeper understanding of the problems has been obtained by the research to date, even more questions have been uncovered. For example, a recurrent problem in the manufacture of explosives is the occurence at ambient temperatures of more than one coexisting crystal phase. This polymorphism is known to occur in TNT, HMX and PbN_3, and is responsible for a degree of behavorial unpredictability, and hence decreases the desirability of these substances as military and industrial explosives.

The total problem of understanding and characterizing explosives and explosive systems is beyond the bounds of any single research effort. In this study the specific problems of TNT polymorphism and phase transitions were researched. This is one of the problems which is relevant to present day concerns.

The experimental techniques which are best suited to solve the current problems associated with explosives must provide a broad probe of these materials. This must be done at a level which, must not only include the atomic and molecular regime, but must also

be sufficiently sensitive to intermolecular interactions so that crystal-phase information can be retrieved. The use of Nuclear Quadrupole Resonance (NQR) spectroscopy is ideal for the proposed investigation. The study of quadrupole coupling constants can provide all of these inputs. Furthermore, even a quick glance at the principal chemical formulae of the explosives of interest will reveal that Nitrogen-14 (nuclear spin =1) ~100% abundant, See Appendix A) is the probe nucleus of choice. Nitrogen-14 NQR is the experimental technique which was used in this research.

2. TECHNICAL DISCUSSION

2.1 NQR SPECTROSCOPY OF NITROGEN

In this Section a brief description will be given of the physical basis of NQR spectroscopy, Appendix A discusses these matters in greater detail.

Nitrogen-14 NQR originates because of the existence of an interaction between the Nitrogen-14 nucleus and the electric field gradient generated by charges in the vicinity of the nucleus. This interaction leads to a quantum mechanical three-level system from which transitions can be induced and detected by conventional spectroscopic methods. The internal nature of the interaction determining the absolute values of the energies involved is the basic reason for the sensitivity of the method to small structural changes. Phase changes involving a change of crystal structure lead to abrupt changes in the frequencies of the NQR spectral lines. This happens because the molecular charge distribution which determines the quadrupolar interaction depends quite sensitively upon the crystalline environment. Phase changes not involving any change in the local crystalline environment are not reflected in the NQR spectral frequencies. They do, however, affect the relaxation times of the transitions.

The spin-lattice relaxation time, T_1, is a macroscopic transport parameter measuring the return to thermal equilibrium of the expectation value of the nuclear spin magnetization.[1] The Hamiltonian coupling the spin system to the lattice is, in general, time dependent through the time dependence of the lattice operators. The

statistical fluctuations of these operators determine the spin-lattice relaxation times. During a phase transition, there are generally large amplitude fluctuations of lattice variables leading to anomalously short spin-lattice relaxation times. In fact, studies of the temperature dependence of the relaxation time T_1 have proven singularly useful in the study of molecular motions and phase transitions [2], and have been shown to yield the direction of the principal axes, thus yielding in a polycrystalline powder much of the information which previously called for single-crystal work [3].

The inverse linewidth relaxation time, T_2^*, is a measure of the inhomogenous line broadening which in turn depends on the degree of disorder of the lattice and on certain molecular motions.

The spin phase memory time, T_2, is a measure of the degree of irreversible loss of transverse nuclear spin magnetization and generally has a singular behavior during critical points.

2.2 PULSED NQR INSTRUMENTATION

Interest in pulsed nuclear quadrupole resonance (NQR) instrumentation has been on the increase as the various advantages of pulsed techniques have become apparent [4-9]. These advantages include: (a) The avoidance of the saturation effects which sometimes plague c.w. spectroscopy, (b) The ability to measure various relaxation times conveniently, (c) The ease with which signal averaging and other data processing can be performed.

The instrument which was used for this research on TNT is principally intended to operate as a Nitrogen-14 NQR research spectrometer and was specifically optimized by Block Engineering for Nitrogen-14 research. It operates in the range 0.5 to 5 MHz. It is capable of producing a rotating magnetic field H_1 of about 20 gauss in a cylindrical

sample 2.5 cm in diameter and 8 cm long. Furthermore, the length of a "$\pi/2$" pulse for a polycrystalline sample [10] in this system is about 50 μsec. The main features of the instrument are,

a. Heterodyne techniques are used throughout.

b. An original matching network design allows one-knob tuning.

c. Choice of several excitation sequences convenient for generation and collection of signals at high data rates is possible.

d. Fast Fourier transform (FFT) routine for studying line-shapes are available.

2.2.1 Block Diagram

Figure 2.2.1-1 is a block diagram of the NQR Spectrometer system. The transmitter and receiver are single conversion heterodyne systems using a fixed frequency local oscillator and a variable frequency master oscillator. A separate sample head contains the transmitter final amplifier, receiver preamplifier, and sample coil matching network. Control of the system and selection of the type of pulse train to be applied to the sample is accomplished with a sequencer unit. The entire spectrometer is located in a well shielded screen room. All output signals are coupled to a remotely located data system by optical isolators. A video terminal and monitor scope used to control the data system and to monitor data system outputs are located adjacent to the screen room.

2.2.2 Transmitter

As shown in the transmitter block diagram (Figure 2.2.2-1) the difference of a 10 MHz crystal controlled local oscillator and a 10.5-15 MHz master oscillator appears at the output of a gated mixer. The master oscillator may be a Marconi R.F. signal generator or a Hewlett-Packard 5100B frequency synthesizer. The local and master oscillator signals, as well as the mixer, are turned on only during the transmitter pulses.

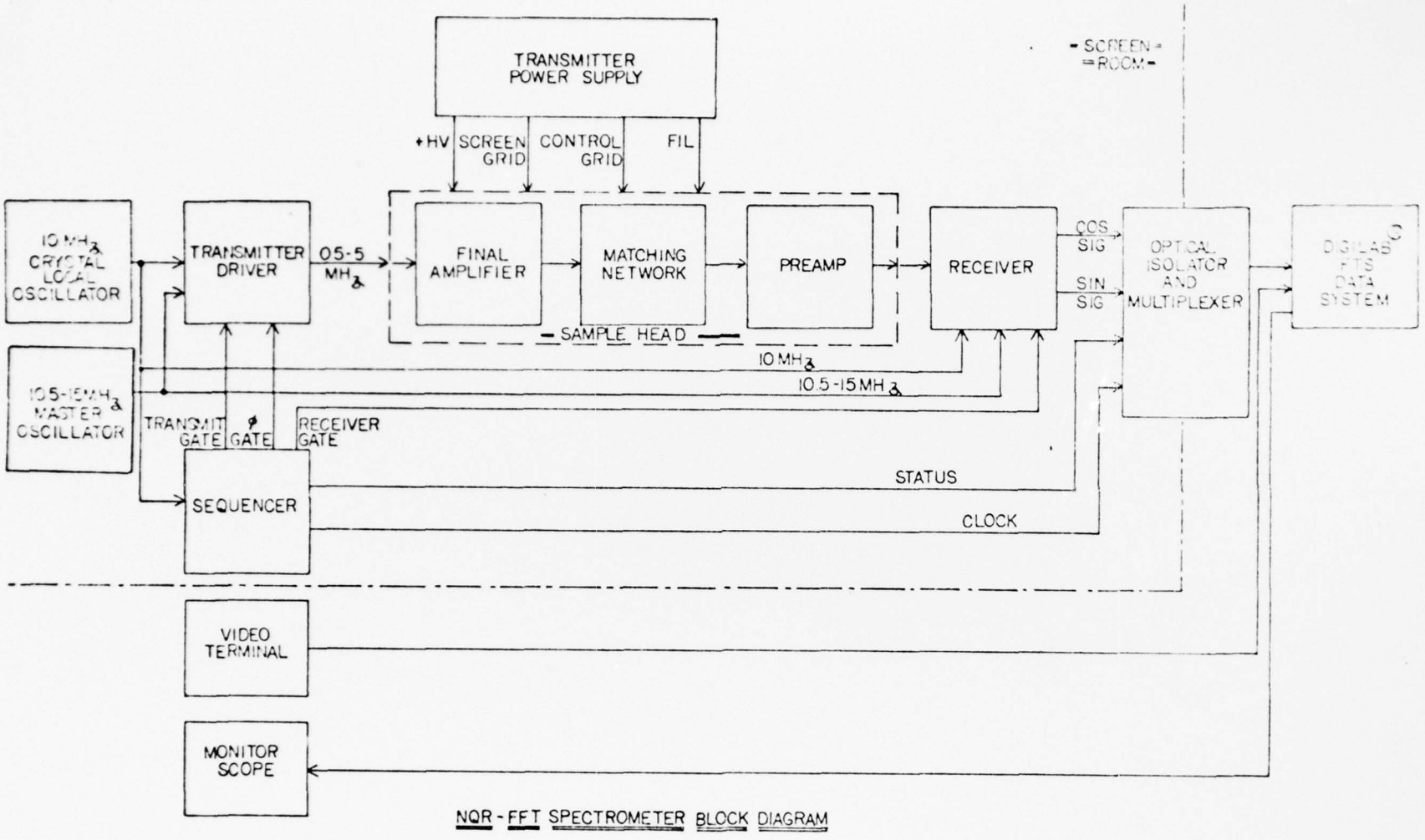

Figure 2.2.1-1 Block Diagram of the NQR/FFT Spectrometer System

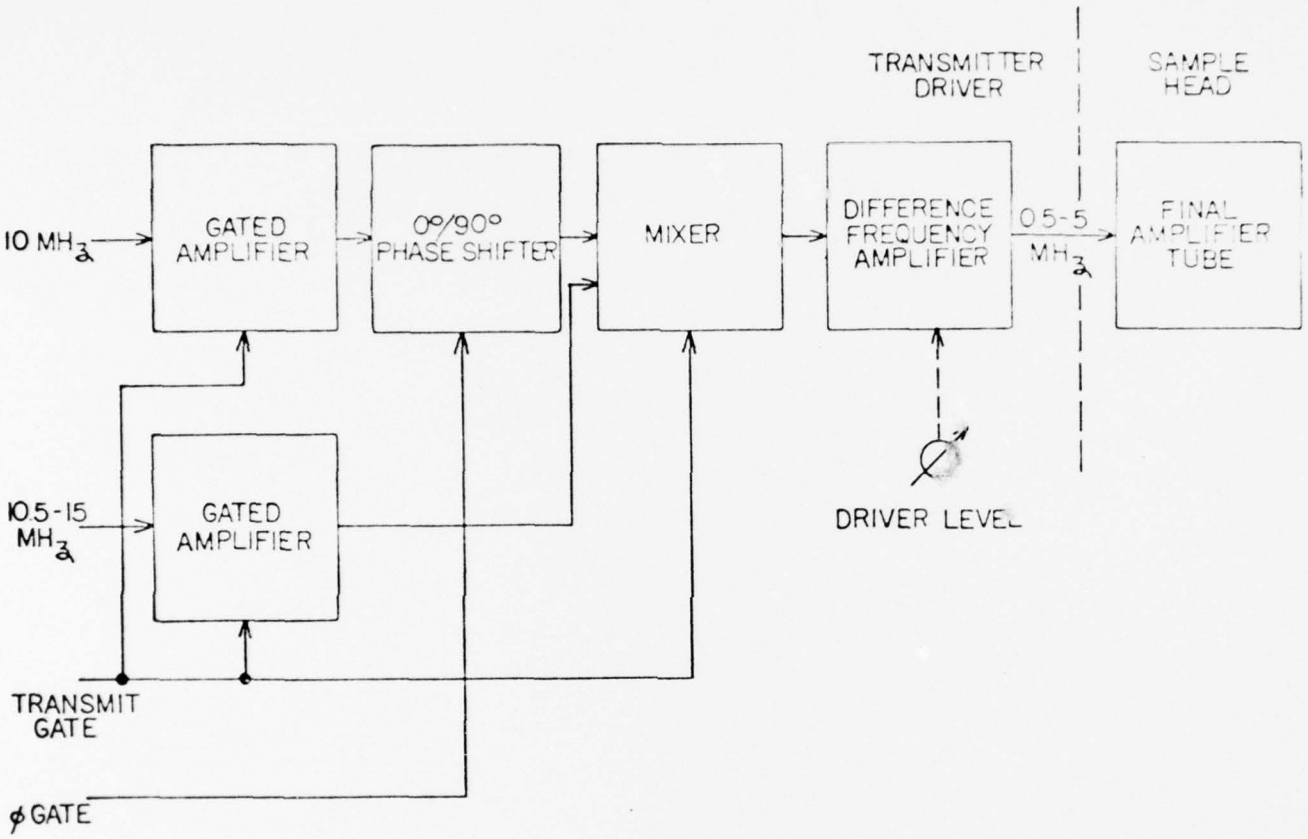

TRANSMITTER BLOCK DIAGRAM

Figure 2.2.2-1 Transmitter Block Diagram of the NQR/FFT Spectrometer

Unlike a homodyne system, this heterodyne procedure prevents any coherent inference signals from being produced in the receiver during NQR signal detection. The phase of the 10 MHz local oscillator may be shifted 90° upon command from the sequencer in order to generate phase shifted sequences such as the Meiboom-Gill modified Carr-Purcell sequence. The difference frequency from the mixer is selected by a low pass filter and then amplified to approximately two watts in order to drive the final amplifier. The final amplifier is a single 4CX250B tube mounted in the sample head operating in class C mode. Operating voltages for the tube are obtained from a separate power supply chassis.

The transmitter voltages and currents are monitored and controlled in the power supply. Variable transformers are used to set the plate screen, and grid voltages. All voltages are heavily filtered to prevent pulse droop from occuring during long pulses or long pulse sequences.

2.2.3 Receiver

The receiver (Figure 2.2.3-1) uses the same oscillators as the transmitter in a heterodyne configuration to detect the NQR resonance signals. The output of a broadband (0.5-5 MHz) preamplifier located in the sample head is mixed with the master oscillator (10.5-15 MHz) in the first mixer of the receiver to produce an intermediate frequency (I.F.) of 10 MHz. The I.F. is built with M1550 integrated circuit amplifiers and double tuned coupling transformers to produce a bandwidth of 20 kHz with a gain of 80 db. A manual I.F. gain control may be used to reduce the gain to 20 db. Since the preamplifier and sample coil tuned circuit greatly attenuate any frequency above 5 MHz, feedthrough of local or master oscillator frequencies is not a problem. Likewise, receiver image frequencies in the 20.5-25 MHz region are also prevented from reaching the receiver mixer.

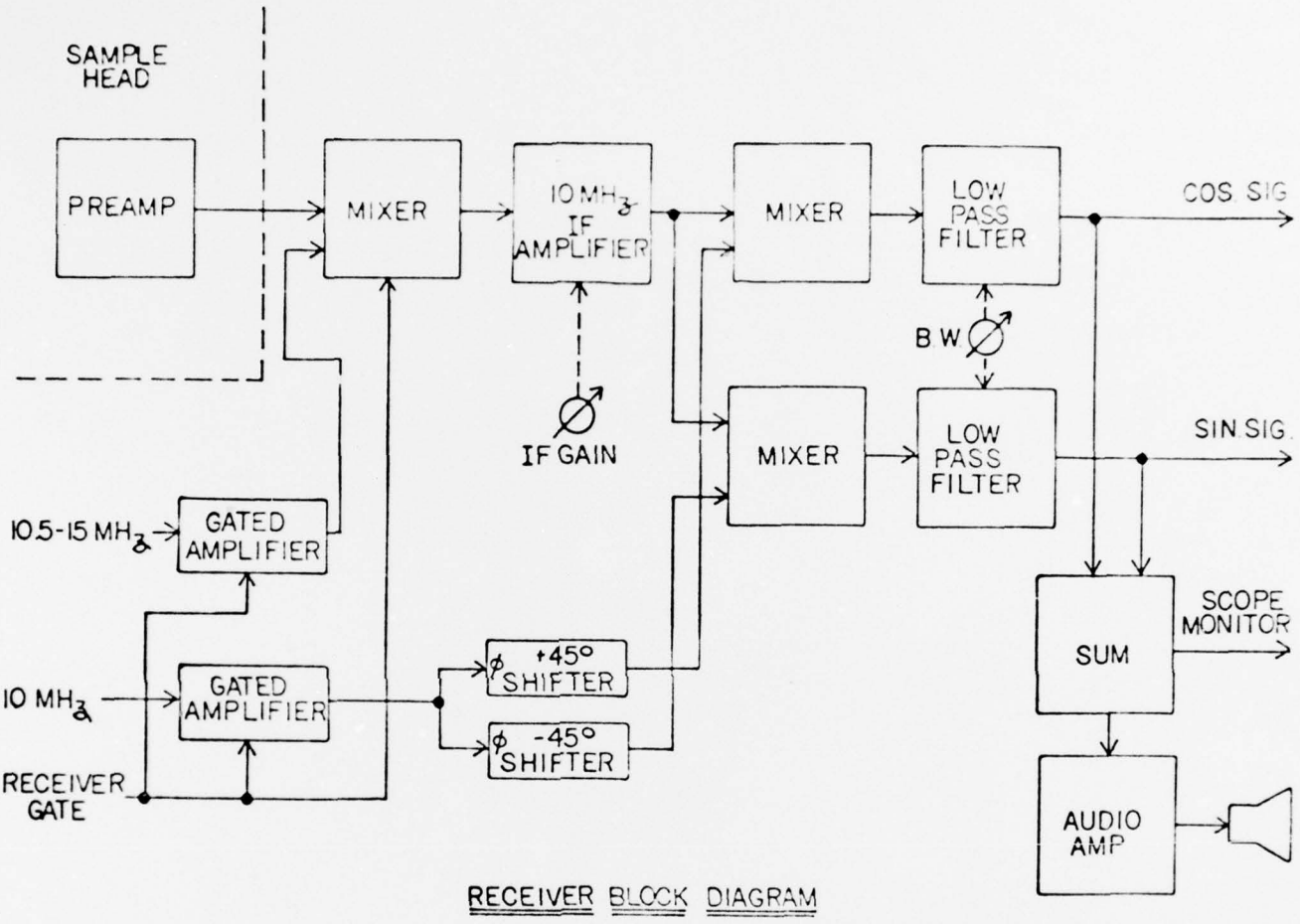

Figure 2.2.3-1 Block Diagram of Receiver Unit of the NQR/FFT Spectrometer

Direct radiation of the 10 MHz local oscillator into the I.F., however, can be a problem unless oscillator levels are kept low and the I.F. is well shielded. The video signal from the I.F. is converted to baseband by two synchronous detectors operating in phase quadrature from the 10 MHz local oscillator. Both the mixer and the synchronous detectors are gated off during each transmitter pulse to achieve fast recovery times by preventing overloading of the receiver. The quadrature detector outputs are filtered by active six pole lowpass filters of 1 kHz, 3 kHz, or 10 kHz bandwidth. Since the outputs of the detectors are DC coupled, no distortion of NQR signals occurs when operating at the exact frequency of an NQR line. An oscilloscope monitor signal is generated by adding the two quadrature outputs. This same signal is fed to an audio amplifier which drives a small speaker in the receiver.

2.2.4 Preamplifier

The preamplifier is mounted in the sample head next to the matching network. This eliminates capacitive loading that would be present with a long coaxial line between the sample coil and the preamplifier and also provides signal amplification with a low impedance output to prevent interference pickup in the line between the preamplifier and receiver. The preamplifier consists of two FET cascode gain stages coupled by an FET source follower, and an FET-bipolar transistor feedback compound that has a low impedance output which drives the twinaxial output cable. The cascode stages use 2N5245 JFET's to produce a gain of 40 db from 0.5 to 5 MHz. In combination with the matching network, the preamplifier increases the Johnson noise equivalent of the sample coil by less than 10%. A pair of back-to-back diodes at the input protect the preamplifier from high RF voltages.

2.2.5 Matching Network

The impedance matching network (Figure 2.2.5-1) used in the spectrometer is designed to allow simultaneous tuning of both the transmitter and receiver by a single control. When searching for unknown resonances this feature is a very convenient one for the operator. In addition, the quality factor Q of the network has the following very useful property. During high voltage R.F. irradiation – transmit mode – the Q of the circuit is very low allowing transmit pulses with fast rise and fall times. On the other hand, in the intervals after R.F. pulses – receive mode – the quality factor Q is high, essentially that of the sample coil itself. As seen in Figure 2.2.5-1, back-to-back diode pairs D1 and D2 are turned on by the high voltage R.F. when transmitting. A resonant circuit is formed by L_1 (the transmitter matching coil), L_2 (the sample coil), and variable capacitor C1. C3 is a large value high voltage DC blocking capacitor which is a short circuit at RF frequencies. The resonant frequency of the transmit circuit is

$$f_{OT} \simeq \frac{1}{2\pi \left(\frac{L1\ L2}{L1 + L2} \times C_1 \right)^{\frac{1}{2}}} \qquad 2\text{-}1$$

with a Q of

$$Q_T \simeq \frac{R_1\ R_2}{R_1 + R_2} \times 2\pi\ f_{OT}\ C_1 \qquad 2\text{-}2$$

In addition to lowering the Q of the transmit mode, R1 prevents excessive screen grid dissipation if L1 is open, and R2 provides a ground return for C3.

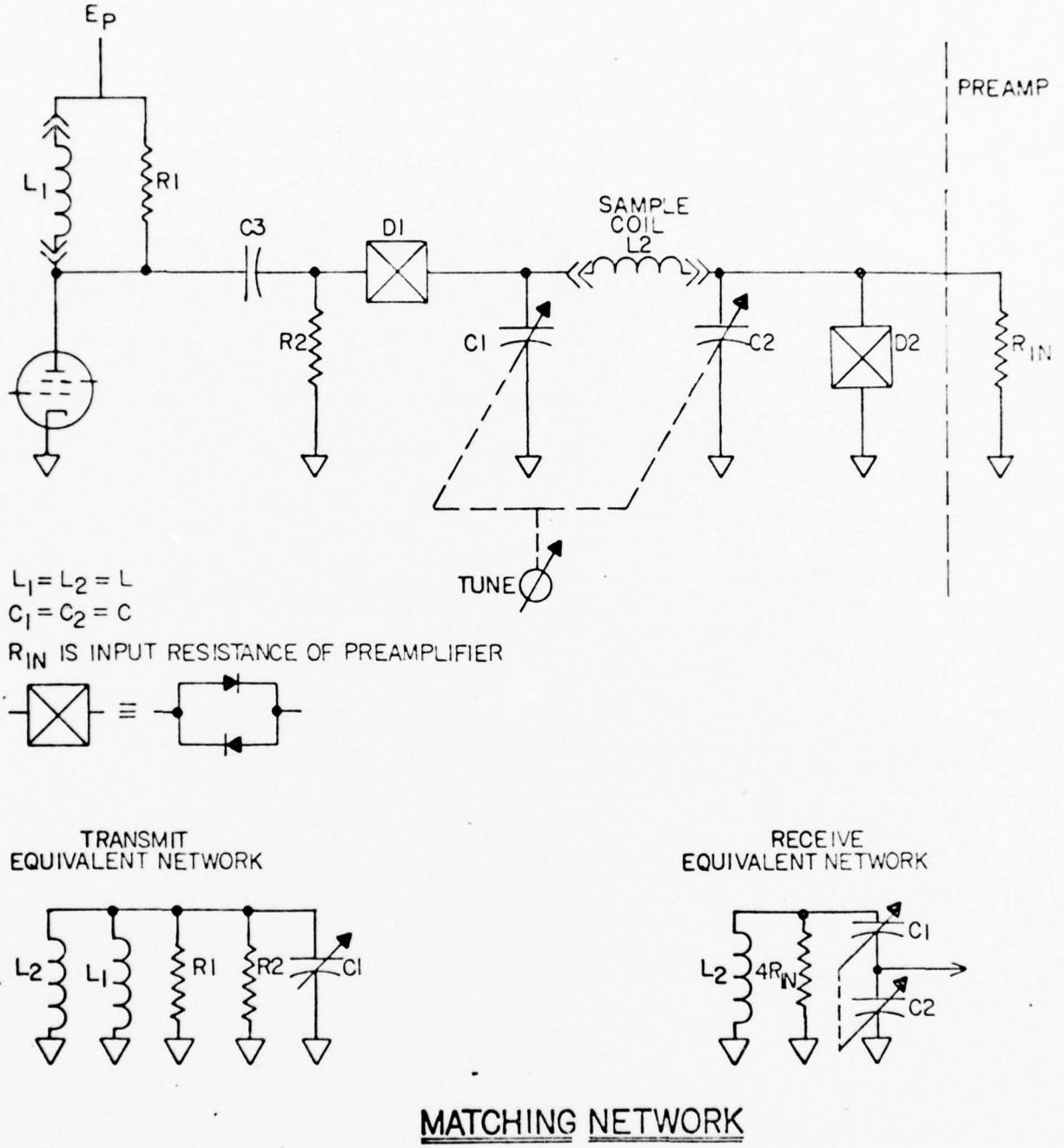

MATCHING NETWORK

Figure 2.2.5-1 Circuit Diagrams for the Impedance Matching Network of the NQR/FFT Spectrometer

When the transmitter pulse ends, the envelope of the R.F. decays with a time constant of $Q_T/\pi f_{OT}$ until the voltage is less than the thresholds of diode pairs D1 and D2. When the diodes stop conducting, the receive mode resonant frequency is

$$f_{OR} \simeq \frac{1}{2\pi \left(L_2 \times \frac{C_1 C_2}{C_1 + C_2} \right)^{\frac{1}{2}}} \qquad 2\text{-}3$$

If C1 and C2 are ganged together so C1 = C2 = C, and if L1 = L2 = L, then

$$f_{OT} = \frac{1}{2\pi \left(\frac{L}{2} \times C \right)^{\frac{1}{2}}} = f_{OR} = \frac{1}{2\pi \left(L \times \frac{C}{2} \right)^{\frac{1}{2}}} \qquad 2\text{-}4$$

and the receiver and transmitter tune simultaneously. The receive-mode Q is determined by the sample-coil Q loaded by the transformed input resistance of the preamplifier. The already high input resistance of the preamplifier input is multiplied by a factor of four by the capacitive voltage divider formed by C1 and C2. In addition, the input capacitance of the preamplifier is absorbed by the much higher value of C2, and capacitive divider C1 and C2 provides a low noise-figure impedance match between the sample coil and the preamplifier.

One limitation of this matching network is that no voltage multiplication takes place between the final amplifier tube output and the sample coil. Thus, the peak-to-peak voltage swing across the sample coil is only twice the plate supply voltage, E_P. The sample coil field strength is

$$H_1 = \frac{E_P}{2\omega} \left(\sqrt{\frac{\mu_o}{V \times L}} \right) \times 10^4 = \frac{E_P}{2} \left(\sqrt{\frac{\mu_{oC}}{V}} \right) \times 10^4 \text{ (gauss)} \qquad 2\text{-}5$$

where V is sample volume in m^3.

The lower limit of the sample coil inductance is set by power losses associated with stray inductances throughout the matching network. The values presently being used in the spectrometer give a value of H_1 of about 20 gauss for a sample of volume of 40 cc.

The ringdown time of the spectrometer is determined by the ringing in the matching network when in the receive mode since the transmit Q is about 5 and the receive Q about 120. At 3 MHz, the ringdown time from 2 volts peak (D2 switching threshold) to 2 microvolts peak (noise floor) is 177 μs plus 4 μs transmit-mode ringdown for a total of 181 μs.

2.2.6 Sequencer

Gating of the transmitter, receiver, and data system is controlled by the pulse sequencer. All sequencer functions are generated from a 100 kHz clock produced by dividing the 10 MHz local oscillator by 100. The pulse widths of the first and second pulses in a sequence are independently set by front panel thumbwheel switches from 10 μs to 1 ms steps. The second pulse may be repeated up to 10,000 times per sequence, and each sequence may be repeated up to 1000 times. After the second pulse, the time between pulses, 2τ, may be set from 1 ms to 100 ms, and the interval between successive sequences may be set from 1 to 10 multiples of one sequence time.

The time between the first and second pulse of a sequence may be set by a mode switch to either 2τ or τ. Another switch may be used to shift the phase of the first pulse by 90° relative to the phase of succeeding pulses. These features allow generation of sequences such as spin echo, Carr-Purcell,[11] Meiboon-Gill modified Carr-Purcell,[12] Spin-Locked Spin-Echo,[13] and a train of $\pi/2$ pulses suitable for FID collection. Typical sequences are illustrated in Figure 2.2.6-1.

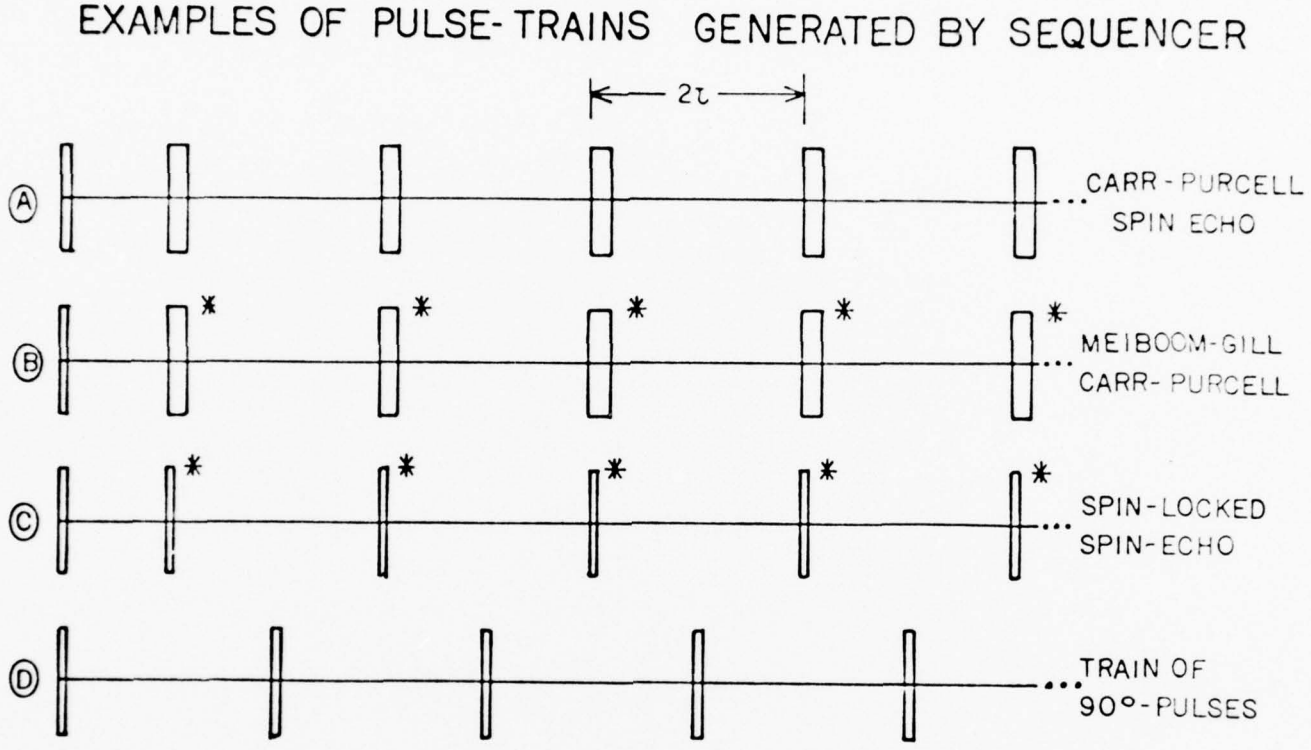

Figure 2.2.6-1 Examples of Pulse Trains Generated by the Sequencer of the NQR/FFT Spectrometer. Thinner pulses denote $\pi/2$ pulses, and thicker pulses denote π pulses.

Gating pulses from the sequencer control the gated mixer and the 90° phase shifter in the transmitter. The receiver gated mixers are turned off during the transmit pulses and for a short time afterwards to prevent the matching network ringdown signal from overloading the receiver. The additional time is set by a ten-turn receiver gate delay control. When the sequencer is not generating pulses, the receiver gate is turned on to allow tuning of the matching network. All gating pulses and internal test points are brought out to test jacks on the sequencer front panel.

The sequencer also generates data system control signals which set the data acquisition clock rate observation times. The clock rate may be set to a frequency of 100 kHz/N where N is an integer between 2 and 20. The status signal (observation gate) allows collection of data either between transmit pulses (event mode) or during the entire pulse sequence (cycle mode). The event mode is used to coherently add either FID's or echoes, and the cycle mode is used for measuring decay times of signal amplitudes.

2.2.7 Data System

The data control signals from the sequencer and the quadrature outputs from the receiver are optically coupled to line drivers which send the signals to the input/output (I/O) modules of a Digilab® FTS data system, Figure 2.2.7-1. The FTS hardware presently being used consists of a NOVA 1200 with 32K word core memory, Digilab® I/O, Digilab® hardware multiply-divide, disc memory, Kennedy tape drive, Houston Complot plotter, and an Infotron video terminal. A Tektronix 465 oscilloscope is used for output monitoring. The Digilab® I/O has a 12 bit A/D converter and hardwired coherent addition capability at rates to 50 kHz.

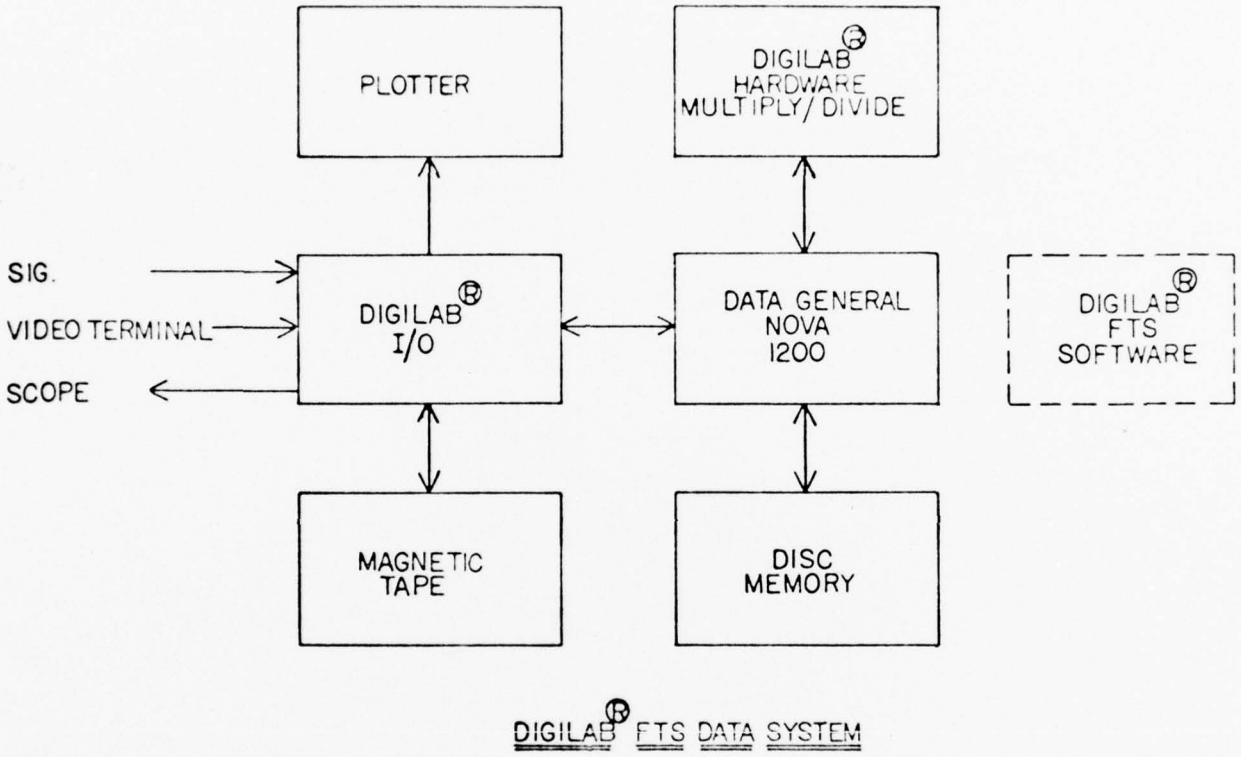

Figure 2.2.7-1 Block Diagram of the Data System with the NQR/FFT Spectrometer

The NQR software system provides for data collection of a number of files with a total capacity of 128K points. Data may also be co-added into these files in real time. This mode is normally used to co-add successive FID's or echoes in order to improve the signal-to-noise ratio. Addition, subtraction, multiplication, or division of two files is also possible. Data files are normally stored for future reference by the magnetic tape unit. Software programs are also loaded by magnetic tape.

A fast Fourier transform (FFT) routine is available for use on FID or echo files. First, a four breakpoint apodization routine is used to minimize the sidelobes of the sampling interval transform and to zero any ringdown time transients at the beginning of the file. An FFT routine may be selected to perform "amplitude only" or real and imaginary transforms of a single receiver output channel. The FFT routine displays on the monitor scope one point in frequency space for every point in the input file. A hardcopy plot of the line-shape with full anotation may then be made, or the transformed data may be stored along with the original data file on magnetic tape. If both quadrature outputs of the receiver are alternately sampled, another FFT routine produces a single sided frequency output with selection between upper or lower sideband. This routine is particularly valuable for analysis of wide lines or closely spaced multiple lines, but requires careful correction for amplitude and phase imbalances between the quadrature channels.

2.3 TYPICAL NQR SPECTRA

The performance of the instrument is best demonstrated by typical spectra which can be obtained. The examples have been chosen to show the versatility of the instrument in evoking and

processing NQR signals. Figure 2.3.-1 depicts the typical response of a sample to the pulse sequences shown in Figure 2.2.6-1a and Figure 2.2.6-1b. Note that in both cases Figure 2.3-1b and 2.3-1c, the response of the spin system is a free induction decay (FID) followed by a series of spin echoes, as expected. All signals are actually "beats" of the nuclear induction signal with the transmitter frequency. The average frequency of the beating is then the distance from exact resonance. The 90° phase shift of all the π pulses of a CP sequence has all the effects which were observed and explained for NMR by Meiboom and Gill in their original paper.[12] First, note that all the signals from the MGCP sequence are in phase, while alternate echoes in the CP sequence are 180° out of phase. Second, errors in the size of the "π" pulses do not produce a cummulative undesirable effect, with the result that the nuclear signal does not decay sooner than is dictated by the spin-phase memory time, T_2. In the case of NQR in polycrystalline powders it is of course impossible to obtain an exact "π" pulse since its value depends on the relative orientation of the sample coil to the electric field gradient principal axes.[10] For this reason alone, the Meiboom-Gill modification to the CP sequence could be recognized as essential for NQR in powdered samples. Quite apart from these considerations, however, the echo train evoked by a MGCP sequence can be much longer than one might expect from the value of T_2 measured a priori. In fact we noticed that as the spacing of the "π" pulses became short relative to T_2, the echo train persists for times of the order of thermal relaxation times. The origin of this effect, whose NMR anology was discovered eleven years ago by Ostroff and Waugh[14] and, independently, by Mansfield and Ware[15] is discussed elsewhere. In Figure 2.3-2 the response to the two sequences, MGCP and SLSE (spin-lock spin-echo) are compared for the ν- line of $NaNO_2$ at 77°K. Note that the SLSE sequence is marginally better at recalling the nuclear magnetization.

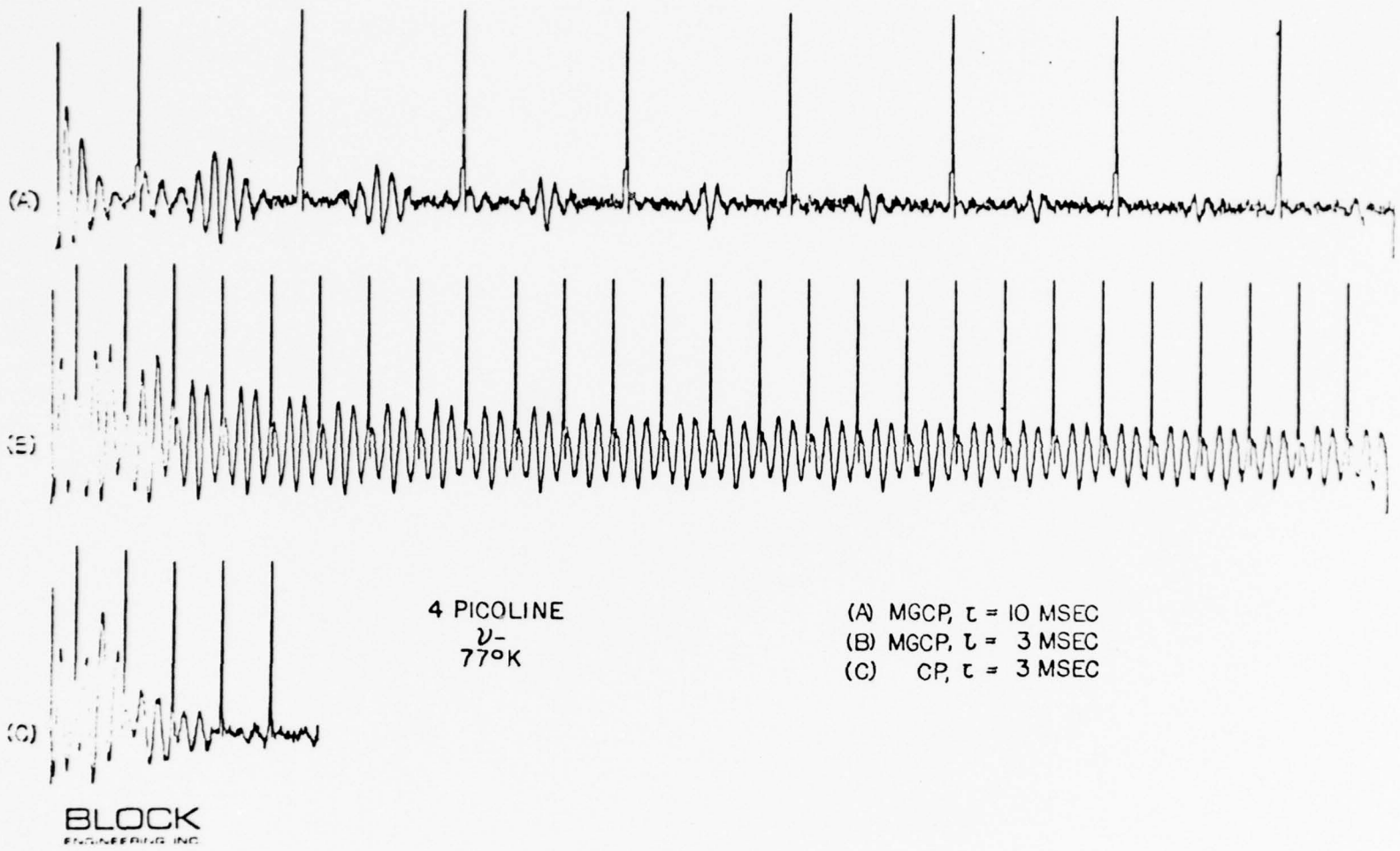

Figure 2.3-1 Signals observed for the ν- line of 4-Picoline at 77°K. The transmitter was offset slightly from exact resonance. Traces (A) and (B) were observed for Meiboom-Gill Carr-Purcell (MGCP) sequences and trace (C) was observed for a single Carr-Purcell (CP) sequence, for the sequence spacing indicated.

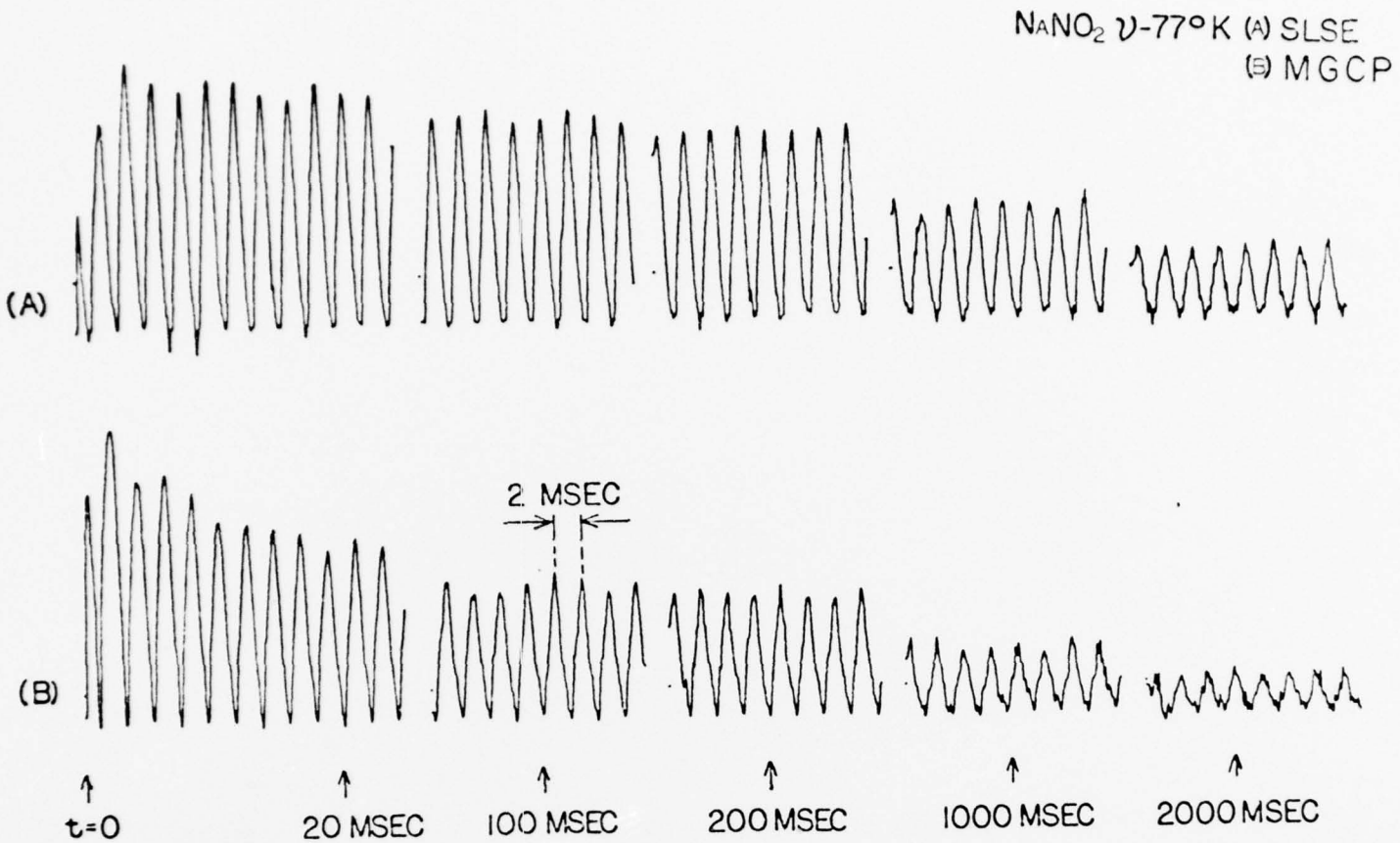

Figure 2.3-2 Signals observed for the ν- line of $NaNO_2$ at 77°K. The spectrometer frequency was set exactly on resonance. The upper trace was obtained from a SLSE sequence, the lower trace was obtained from a Meiboom-Gill modified Carr-Purcell sequence.

For the purpose of enhancing the signal-to-noise ratio of an NQR line, either to aid in its detection or to facilitate line shape studies, the SLSE sequence can offer the kind of fast data rates previously only achieved in systems with thermal relaxation times as short as a few milliseconds. The upper traces in Figure 2.3-3 and Figure 2.3-4 show examples of NQR signals obtained by coherently adding the spin echoes in a SLSE sequence. The lower traces are amplitude Fourier transforms of the time-domain echo signals and hence represent the line shapes of the respective NQR lines. Two more interesting line shapes are shown in Figure 2.3-5 and Figure 2.3-6. Figure 2.3-5 is the amplitude Fourier transform of one spin echo for the ν_+ line of urea at 77°K. The line shape "bump" on the low frequency side is a reproducible feature and is conjectured to be due to proton-N^{14} dipolar coupling in this strongly hydrogen-bonded system. Finally, Figure 2.3-6 shows the Lorentzian lineshape and splitting[16] of hexamethylenetetramine. This results from the Fourier transform of the time-domain signal coherent sum of FID signals collected using the sequence shown in Figure 2.2.6-1d.

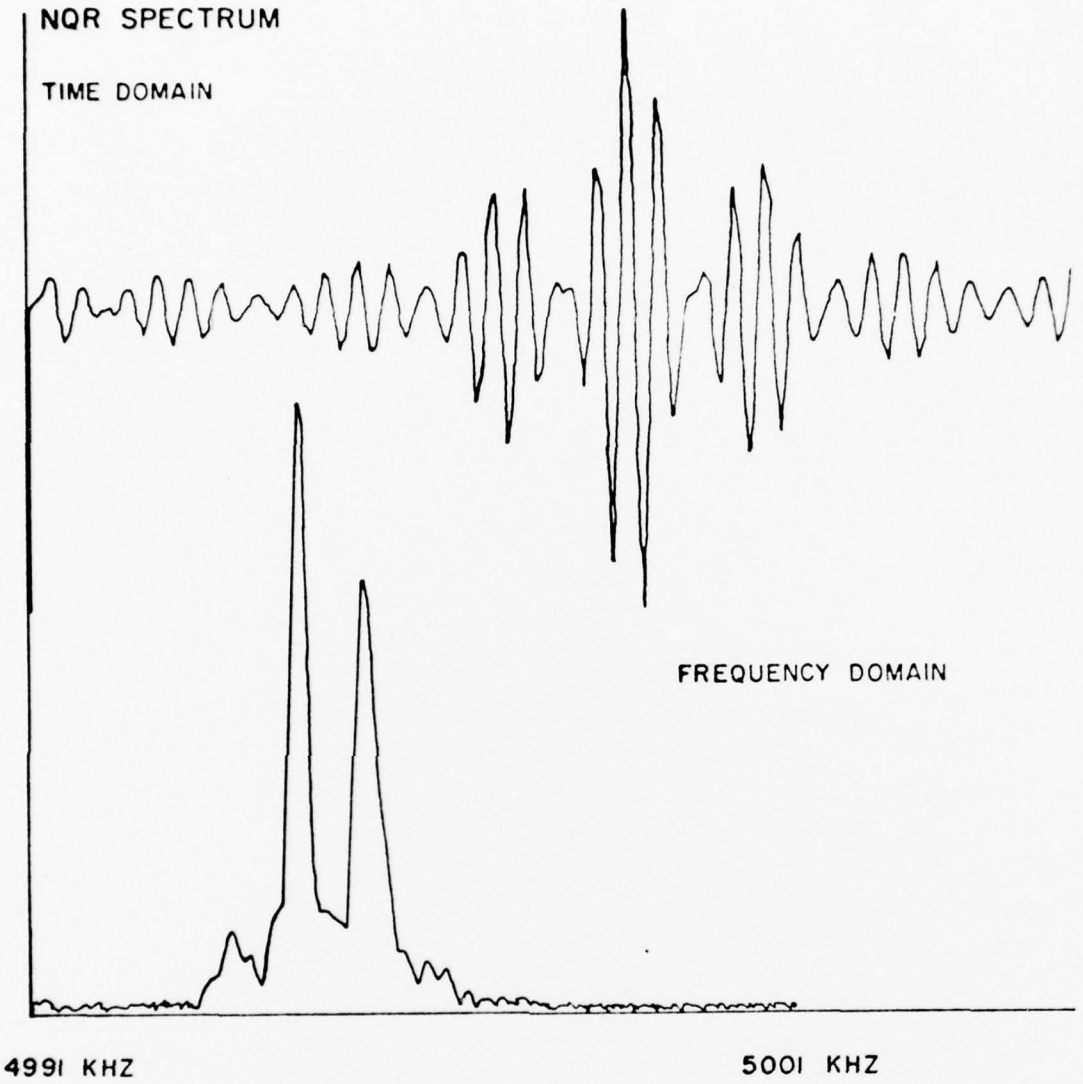

Figure 2.3-3 The time domain echo signal and its Fourier transform for N,N - Dimethylhydrazine at 77°K. NQR lines in this example are particularly narrow.

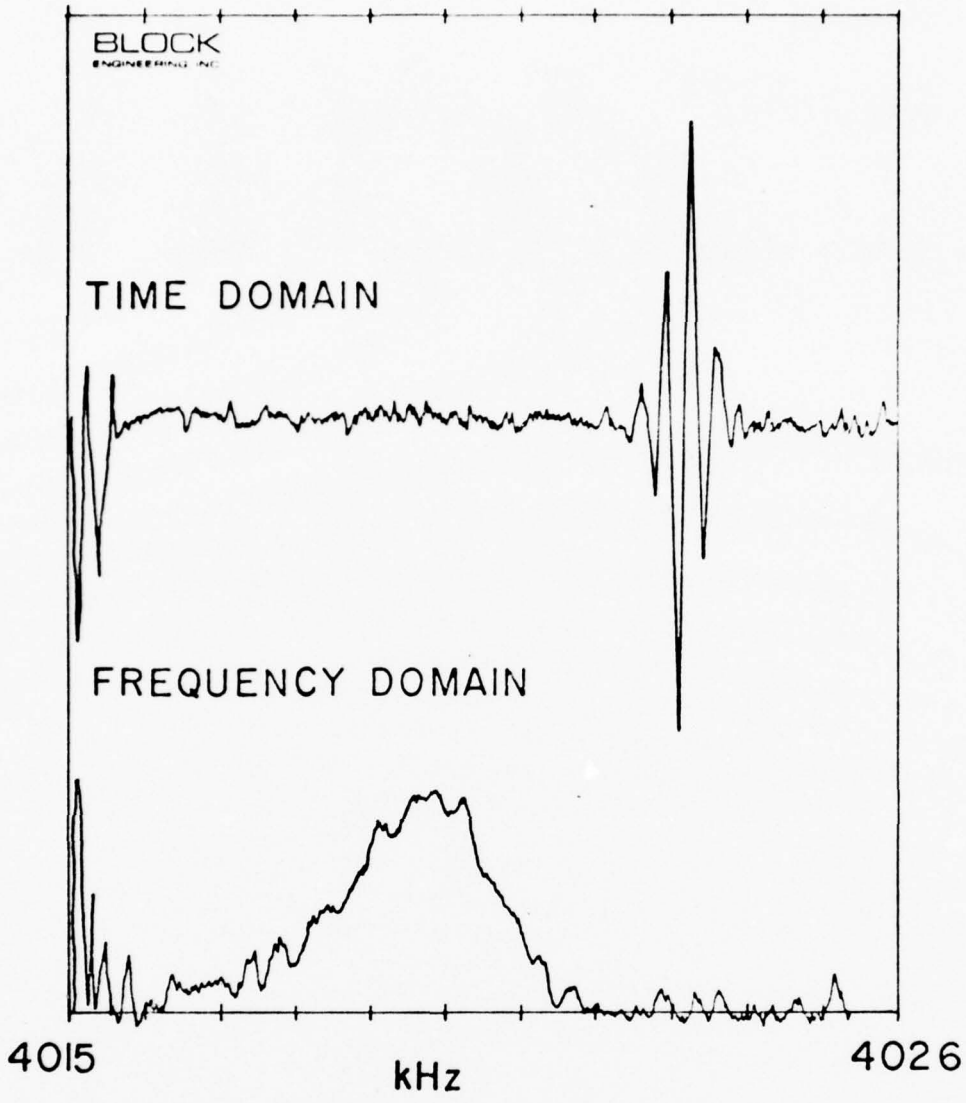

Figure 2.3-4 The time-domain echo signal and its Fourier Transform for N,N-Dimethylanaline contaminated with water. Data obtained at 77°K and exemplifies a particularly broad NQR line.

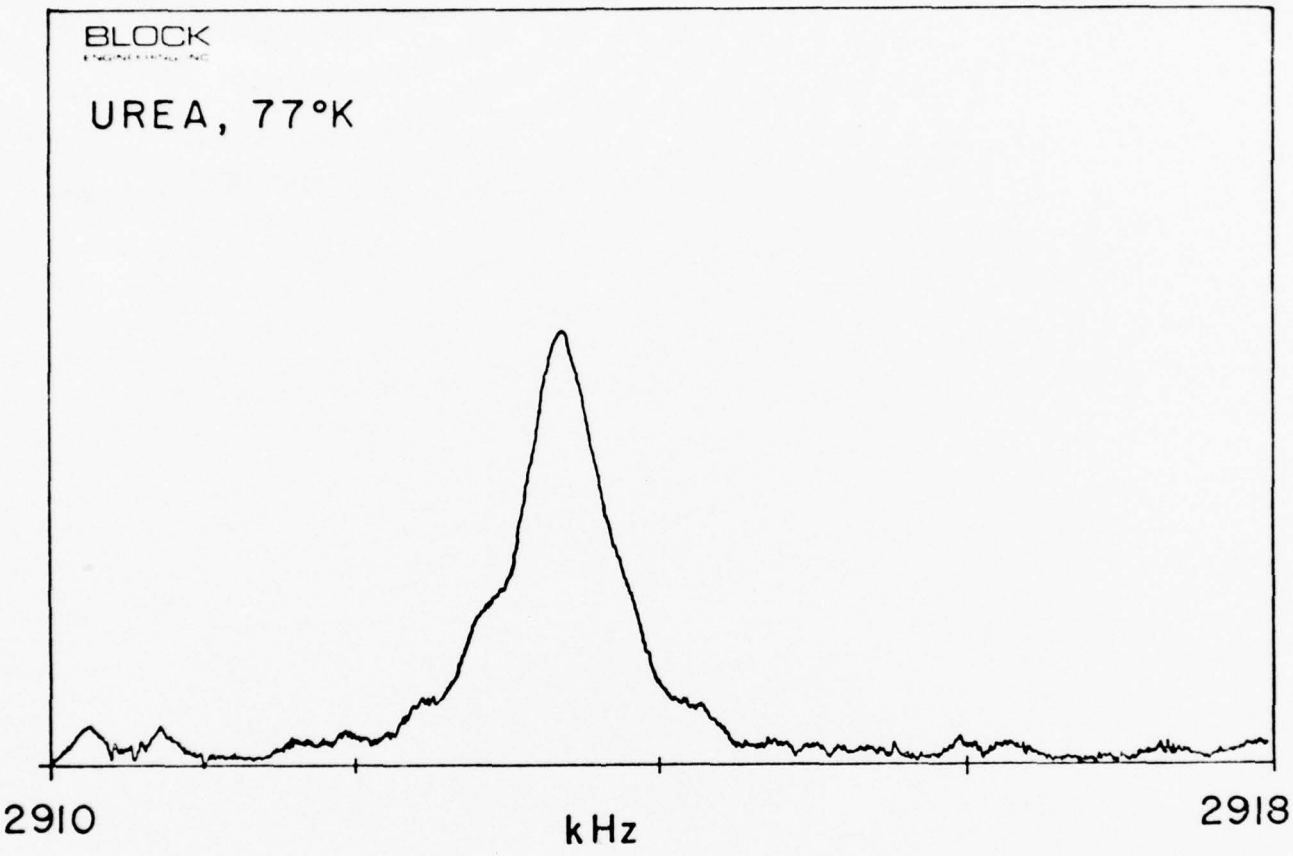

Figure 2.3-5 Amplitude Fourier transform of one echo for the $\nu+$ line of urea at 77°K. The broad feature on the low frequency side is reproducible.

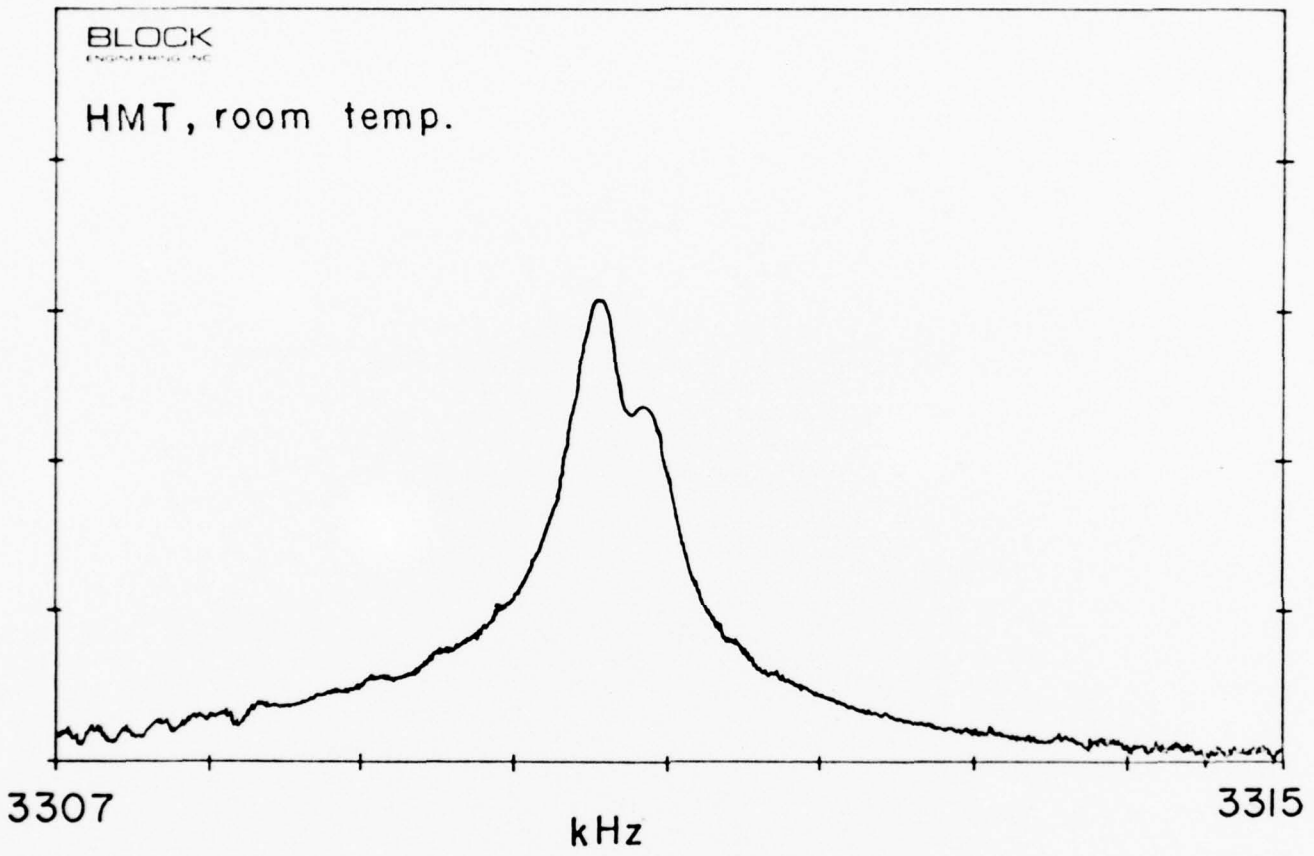

Figure 2.3-6 Amplitude Fourier transform of coherently added Free Induction Decay (FID) signals in Hexamethylenetetramine at room temperature. Note resolved doublet structure.

3. MULTIPLE PULSE SPIN-LOCKED SPIN-ECHO TECHNIQUES

3.1 GENERAL

In the course of the NQR work on TNT characterization, a novel effect was observed which greatly enhanced the sensitivity and versatility of the pulsed NQR/FFT system. Although this effect, multiple pulse spin-locked spin-echo, is, in general, very useful for NQR spectroscopy, it is of particular value in the present TNT studies because weak room temperature resononances can be observed. In fact, a reasonable part of this research was devoted to characterizing this phenomenon [13] so that the very weak room temperature lines of TNT could be accurately measured. The importance of this finding is pointed out in the discussion which follows.

Wider use of Nitrogen-14 nuclear quadrupole resonance (NQR) as a research tool has long been hampered by the relatively poor signal-to-noise ratio obtained from typical samples. In addition, generally long spin-lattice relaxation times have prevented efficient signal averaging. A number of double resonance techniques[17-20] have been successfully used to attempt to improve sensitivity, but they suffer from considerable instrumental complexity.

The present research resulted in the observation of an effect which promises to improve substantially the effective sensitivity of N^{14}NQR in typical samples without recourse to complicated double resonance schemes. In fact the improvement is enhanced by the existence of long thermal relaxation times. The effect, which appears to be completely analogous to that observed in nuclear magnetic resonance (NMR) eleven years ago by Ostroff and Waugh[14] and by Mansfield and Ware[15], naturally lends itself to efficient data processing. The spectrometer which was used to perform these experiments was described in Section 2.2.

Figure 3.1-1 depicts a typical manifestation of the phenomenon. A modified Carr-Purcell [11] sequence applied on resonance to a pure quadrupole resonance transition in $NaNO_2$ evokes in response a train of spin echoes which persists for seconds even though the spin-spin relaxation time T_2 measured by the 90°-τ-180° method is only 8×10^{-3} sec. The unexpected persistence of the echo train for times much greater than T_2 occurs when $\tau \leq T_2$, where τ is the time spacing between the first two pulses of the excitation sequence, and when the Carr-Purcell sequence is modified in the following two ways: (a) All the pulses are 90° pulses [21] and (b) The first pulse is phase shifted by 90° with respect to all the others. Under these conditions the spin-echo train decays as the sum of two exponentials, a result not unexpected in a three-level system. In what follows the longer of the two relaxation times,[22] is labeled $T_{2\varepsilon}$. For $\tau \leq T_2$, the effective relaxation time $T_{2\varepsilon}$ becomes strongly dependent on τ. Figure 3.1-2 shows the dependence of $T_{2\varepsilon}$ on τ for the ν- line of $NaNO_2$ at 77°K. Note that for $T_2 < T_{2\varepsilon} < T_1$ the data are fit very well by the relation[24,25], $T_{2\varepsilon} \sim \tau^{-5}$, lending strong support to the contention that what is being observed is spin-locked pure quadrupole resonance spin echoes. If so, one would then expect that for $\tau \to 0$ one would obtain $T_{2\varepsilon} \to T_{1\rho}$, the spin-lattice relaxation in the rotating frame. However, no independent measurements of $T_{1\rho}$ are available to check this last hypothesis.

The size of the sensitivity enhancement that is made possible by coherently adding the individual echoes within each spin-locked spin-echo (SLSE) sequence is easily shown to be a factor of $0.64\ z^{1/2}/(i-e^{-z})$, where $z = 2\tau/T_{2\varepsilon}$. This enhancement is obtained by coherently adding the optimum number of echoes, approximately $1.26/z$. For example, for an NQR signal with $T_{2\varepsilon}$ = 10 sec it is possible to improve the sensitivity by a factor of 64 over the single-shot signal by co-adding the first 12,600 echoes in a SLSE sequence with τ=500 μsec.

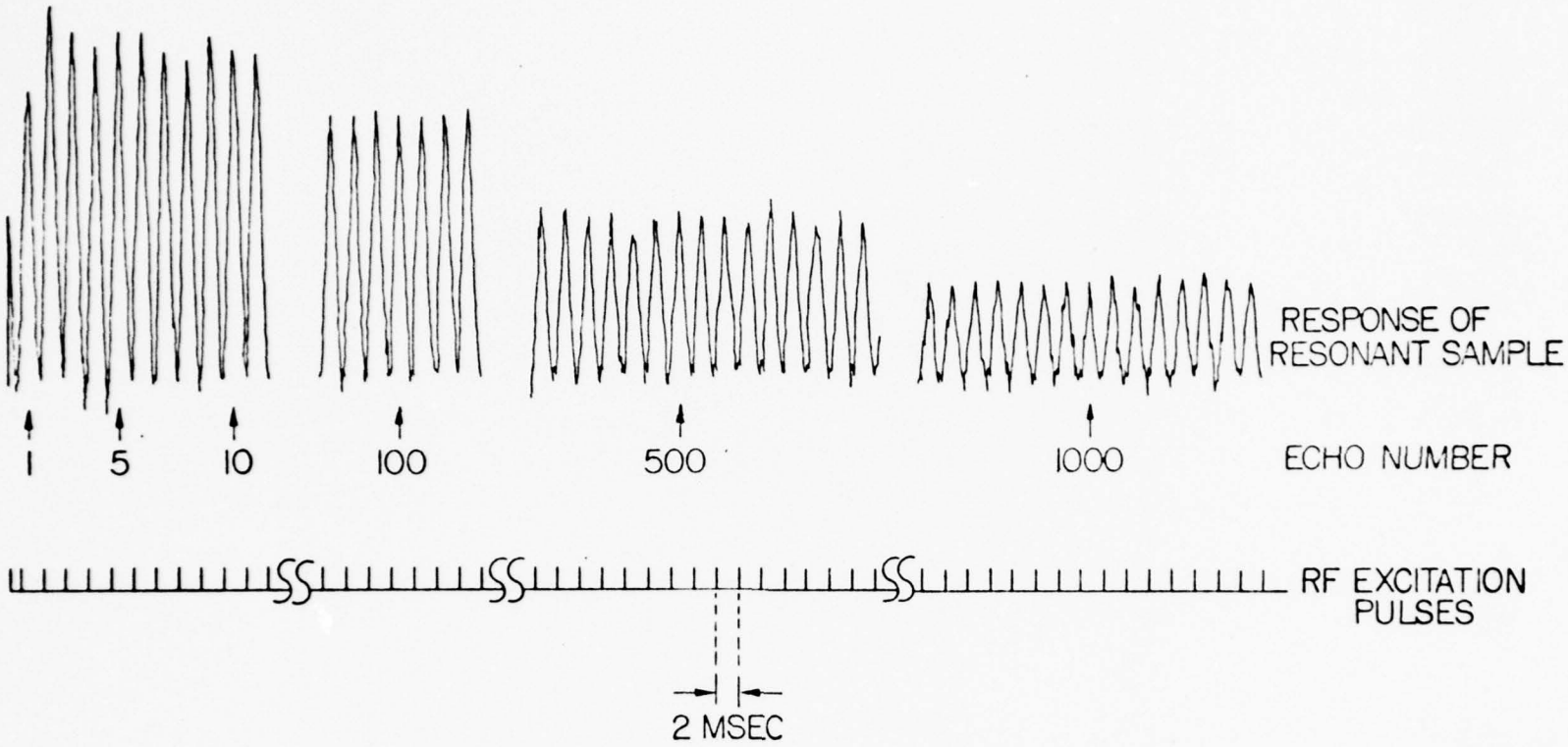

Figure 3.1-1 Spin-locked spin-echo train in $NaNO_2$. The lower trace depicts the modified Carr-Purcell sequence described in the text. The upper trace shows portions of the resultant echo train. The sample consists of 40 grams polycrystalline $NaNO_2$ at 77°K. The transition is the ν- NQR line at 3757 kHz.

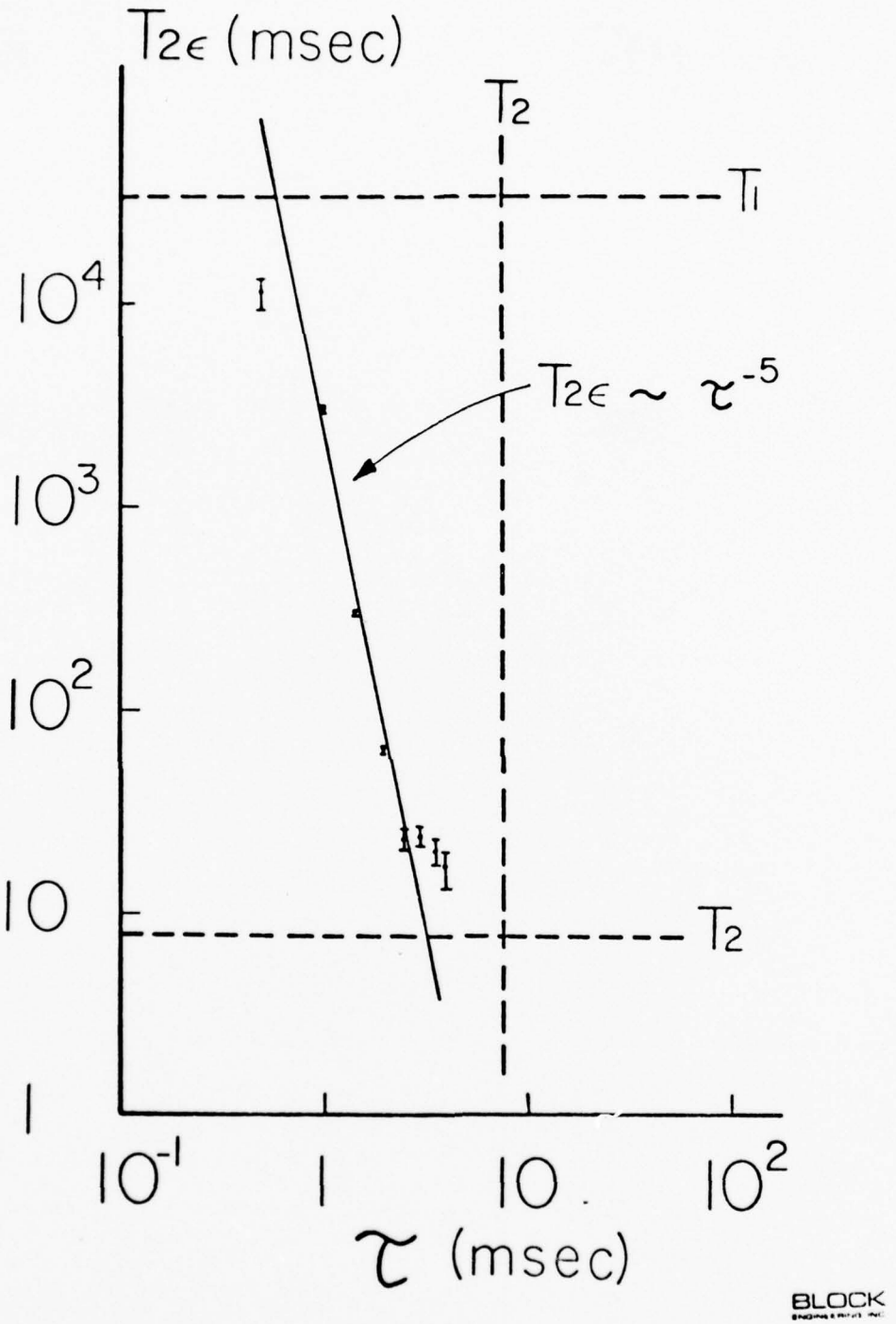

Figure 3.1-2 Double logarithmic plot of the decay constant $T_{2\varepsilon}$ of the echo train in a SLSE sequence vs. the spacing τ between the first two pulses of the sequence. Data obtained for the ν- line of $NaNO_2$ at 77°K.

In an actual experiment which approximates this situation 350 mg. of $NaNO_2$ were easily detected (signal-to-noise ~10, at 77°K) by co-adding 10^4 echoes generated in 10 seconds in a single SLSE sequence.

Finally, it is conjectured that by operating in the region where $T_{2\varepsilon}$ is strongly dependent on τ (c.f Figure 3.1-2), the sensitivity of the double resonance scheme of Emshwiller, Hahn, and Kaplan[26] can be greatly enhanced.

3.2 ADVANTAGES AND LIMITATIONS

Figures 3.1-2, 3.2-1, and 3.2-2 show a double logarithmic plot of the effective spin-phase memory time $T_{2\varepsilon}$ vs the parameter τ the spacing between the first two pulses in the spin-locked spin-echo (SLSE) sequence. These results are, respectively, for the ν_- line of sodium nitrite at 77°K, for sodium nitrite at room temperature, and for 4-picoline at 77°K. These particular compounds were chosen to give a varied sampling of T_1 and T_2 values. Note that a general pattern emerges, which can be summarized as follows. As SLSE sequences of progressively small τ values are employed, the echo-train decay constant, $T_{2\varepsilon}$, remains close to T_2 for $\tau \geq T_2$. For $\tau < T_2$ it is observed that $T_{2\varepsilon}$ begins to increase dramatically, and continues to do so until it "saturates" when $T_{2\varepsilon} \approx T_1$. It should be noted that since $T_{1\rho}$ has not been measured for any NQR line the assumption is made that $T_{1\rho} \approx T_1$ for purposes of this discussion. It should be pointed out that only in the first case, $NaNO_2$ at 77°K, where the ratio T_1/T_2 is largest, is $T_{2\varepsilon} \approx \tau^{-5}$ as predicted by theory. For the other two cases the dependence of $T_{2\varepsilon}$ on τ^{-n} is closer to n = 2 or 3 than to 5. It remains to be discovered, by further theoretical and experimental work, whether a different power law can in fact be dominant, or whether what is observed is the effect of a too low T_1/T_2 ratio to allow the τ^{-5} dependence a sufficient range to show itself.

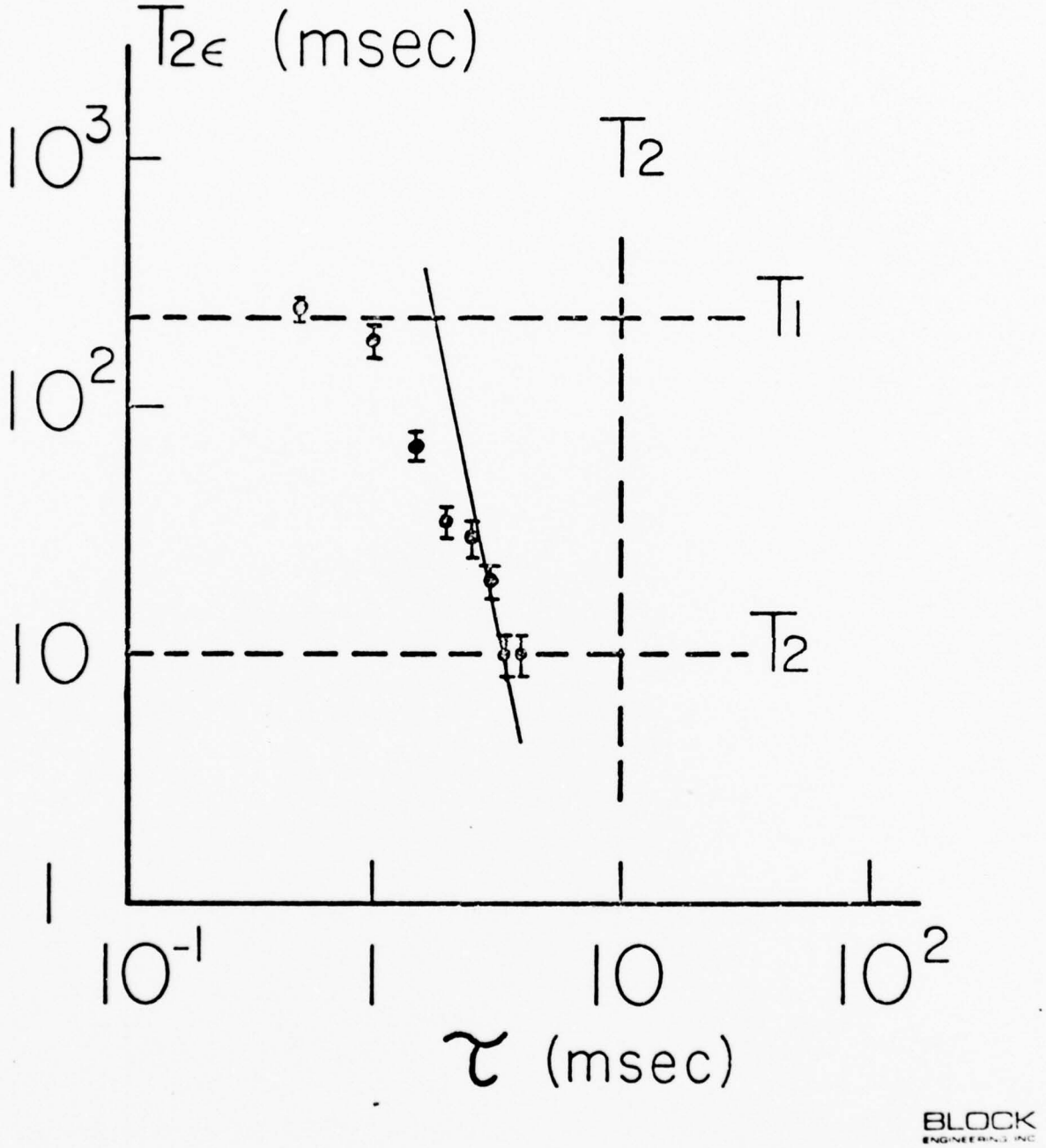

Figure 3.2-1 Double logarithmic plot of the decay constant $T_{2\varepsilon}$ of the echo train in a SLSE sequence vs. the spacing τ between the first two pulses of the sequence. Data obtained for the ν- line of $NaNO_2$ at room temperature.

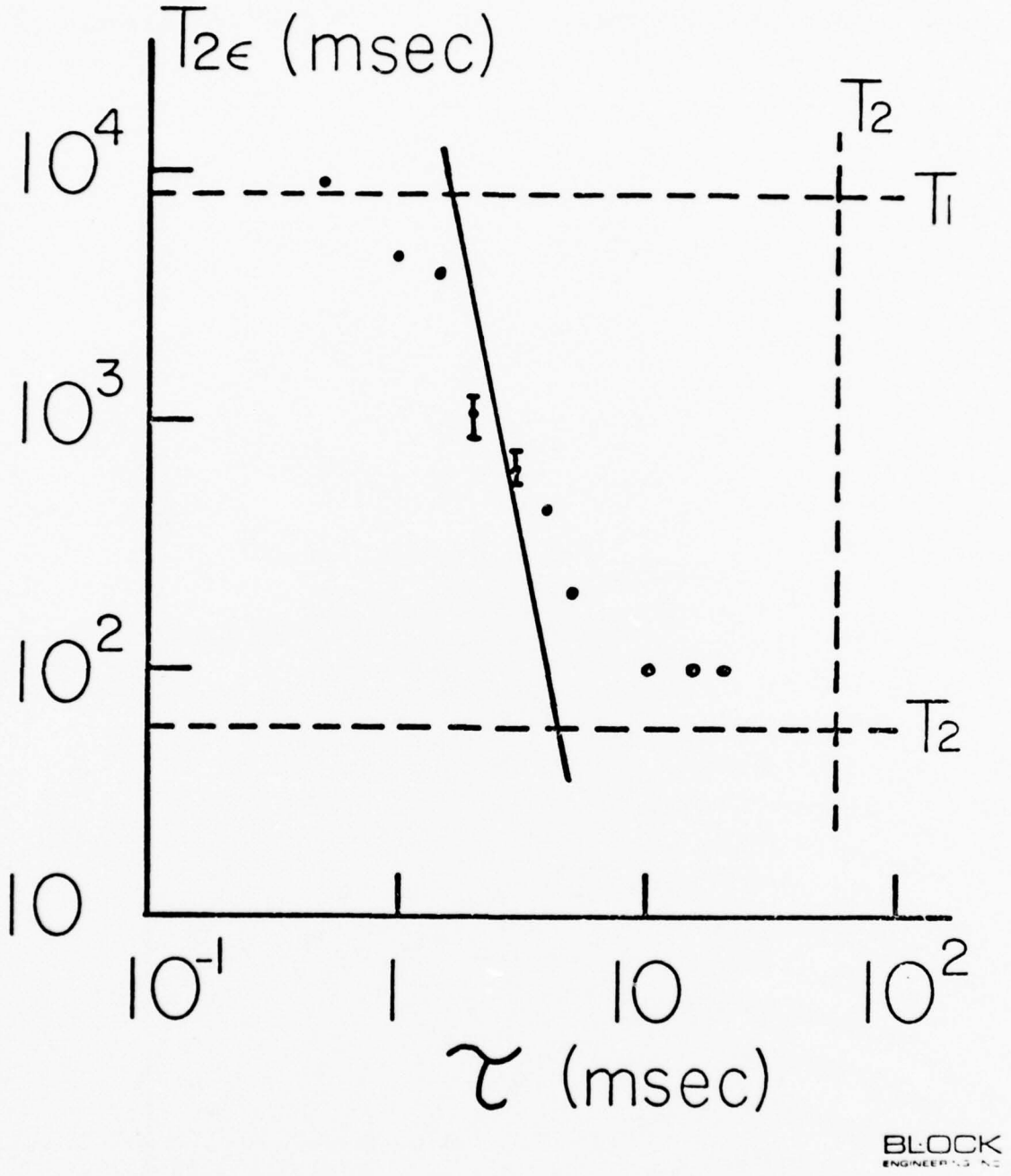

Figure 3.2-2 Double logarithmic plot of the decay constant $T_{2\varepsilon}$ of the echo train in a SLSE sequence vs. the spacing τ between the first two pulses of the sequence. Data taken for the ν- line of 4-Picoline at 77°K.

For the purposes of this report, therefore, it must be pointed out that the spin-locked spin-echo technique for fast data rate production and collection becomes less efficient for low values of the ratio T_1/T_2. For low values of T_1 conventional signal averaging comes into its own and it is precisely for large values of T_1 that a need for more efficient signal averaging exists, and is addressed by the SLSE method.

4. SMALL SAMPLE TECHNIQUE; FERRITE CORES

4.1 OBJECTIVE

Nuclear magnetic resonance (NMR) and nuclear quadrupole resonance (NQR) have traditionally been observed by placing the sample material inside a coil, or coils, which served to excite the resonance and monitor the response of the nuclear spin system. It is clear that the signal strength in such a case depends, among other parameters, both on the number and kind of resonant spins present and on the electromagnetic coupling between the exciting/receiving coil(s) and these spins. This concept has often been summarized under the "catchall" phrase, "filling factor". The geometry of the sample coil is dictated, to a large extent, by considerations having to do with its inductance, so the desired frequency and the magnitude of the electromagnetic field, which must be generated inside the coil proper can be attained. The optimum strategy, so far, has, therefore, been to design sample coils which satisfy the electronic constraints while maximizing the sample volume in the frequency region of interest. Thus, c.w. or pulsed NQR spectrometers operating in the low MHz range e.g. Nitrogen-14 NQR spectrometers, use sample volumes of the order of 10-100 cm^3. The unstated assumption so far has been that there must be a sufficient amount of sample material to completely fill these coils. Alternatively it is assumed that it is possible to wind a sample coil of satisfactory quality factor, Q, and other electronic characteristics around the available amount of sample while maintaining a high value for the filling factor. These assumptions break down when the sample volume is of the order of 1 cm^3 or less. Furthermore, when the search frequency tends towards the low end of the spectrometer frequency range it becomes increasingly difficult to wind a sample coil of sufficiently high inductance, high quality factor Q and low volume.

4.2 PRELIMINARY DATA

In an effort to avoid the conflict between "filling factor" and sample size (< lcc) the following scheme was investigated. Taking advantage of the fact that no external static magnetic field is applied to the sample in the course of a pure nuclear quadrupole resonance experiment, ferrite material was used in a geometry such as is shown in Figure 4.2-1. Ferrite material with an initial permeability of 125, and low loss at below 5 MHz frequency is available from several manufacturers. The advantages of this scheme are two fold

a. High inductance/low sample-volume coils can be wound with no difficulty.

b. The coupling of the resonant spins to the receiving coil is greatly enhanced.

Applications of this technique are envisioned for situations where only small amounts of sample are available for econimic or technical reasons, e.g. small single crystals of subtances whose crystal habits prohibit larger crystals, or high sensitivity explosive materials where large amounts might pose a safety hazard.

The following experiments were performed to determine the practicality of these conjectures. Two gapped toroids of Q1 ferrite material were purchased from Indiana General Corporation. The dimensions of the two coils studied are shown in Figure 4.2-1. In each case a coil was wound so as to obtain an inductance value of 42 μH, equal to that of a control air core sample coil of standard dimentions (2.5 cm diameter by 8 cm tall). The following conclusions were drawn by observing NQR signals in sodium nitrite ($NaNO_2$) and hexamethylenetetramine (HMT) at room temperature.

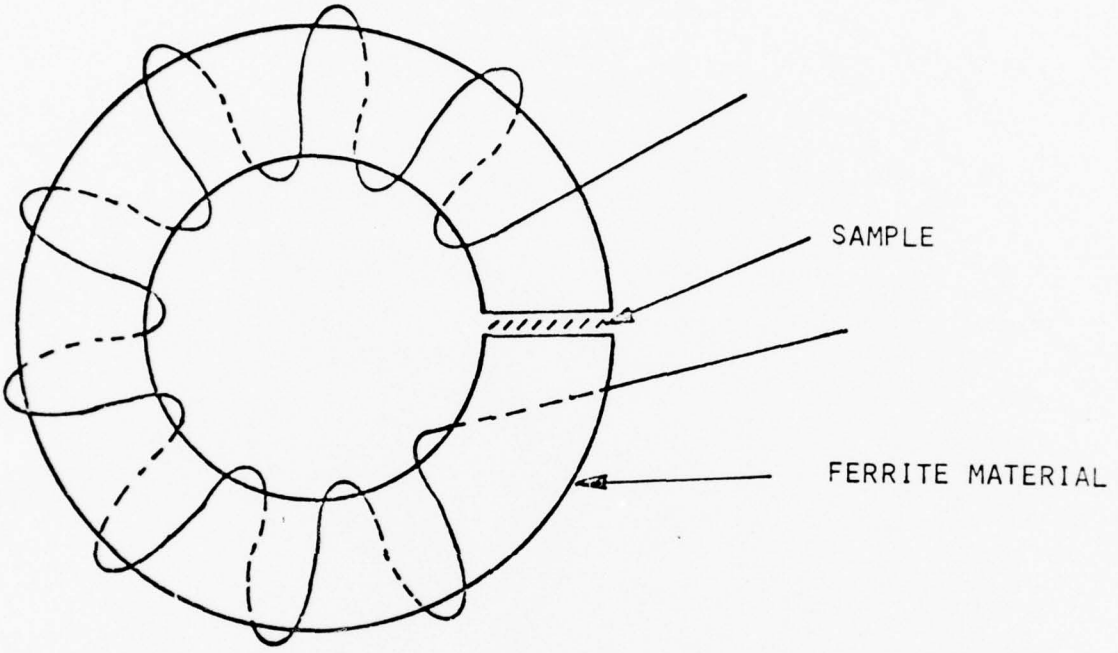

Coil Size / Dimensions	Small	Large
inner diameter	2 1/4 in	2.5 in
outer diameter	3 in	5.75 in
width	0.5 in	0.6 in
gap length	1/16 in	3/32 in

BLOCK
ENGINEERING INC

Figure 4.2-1 Geometry and Dimentions of Ferrite Coils

4.2.1 Advantages of Ferrite Coil Technique

The ferrite coil research led to some very promising preliminary results. These include

a. Small Samples contained in the toroid gap could be excited to satisfactory levels so that they exhibited spin-echoes.

b. The coupling of the resonant nuclear spins to the sample coil appear to have been considerably improved in actual practice because the signal-to-noise ratio of spin-echoes from the ferrite assembly were 5-7 times better than when corresponding amounts of material were dispersed in a 40 cc sample bottle and detected with the air-core coil. This observation vindicates the basics of the ferrite conjecture as can be seen from Figure 4.2.1-1.

4.2.2 Drawbacks of the Ferrite Coil Technique

Preliminary information indicate that there are disadvantages to the ferrite coil approach. Some of these can probably be overcome with additional research. The following is a summary of the perceived disadvantages of ferrite core sample coils:

a. Because of the unfavorable temperature dependence of the permeability of the ferrite material, only the region close to room-temperature is accessible for experiments.

b. Because of the ferrmagnetic nature of the ferrites a remanent magnetic field is present in the gap even when no RF pulse is being applied. This DC field has the effect of broadening NQR lines in polycrystalline samples. The degree to which this happens depends critically on the parameter $\eta(e^2qQ)$, where η = asymmetry parameter and e^2qQ = quadrupole coupling constant e.g., In $NaNO_2$, with $\eta e2qQ \approx 2MHz$, the signal is barely perturbed at all, while in HMT, with $\eta e^2qQ \approx$ zero, the signal was UNOBSERVABLE (down by at least 2 orders of magnitude).

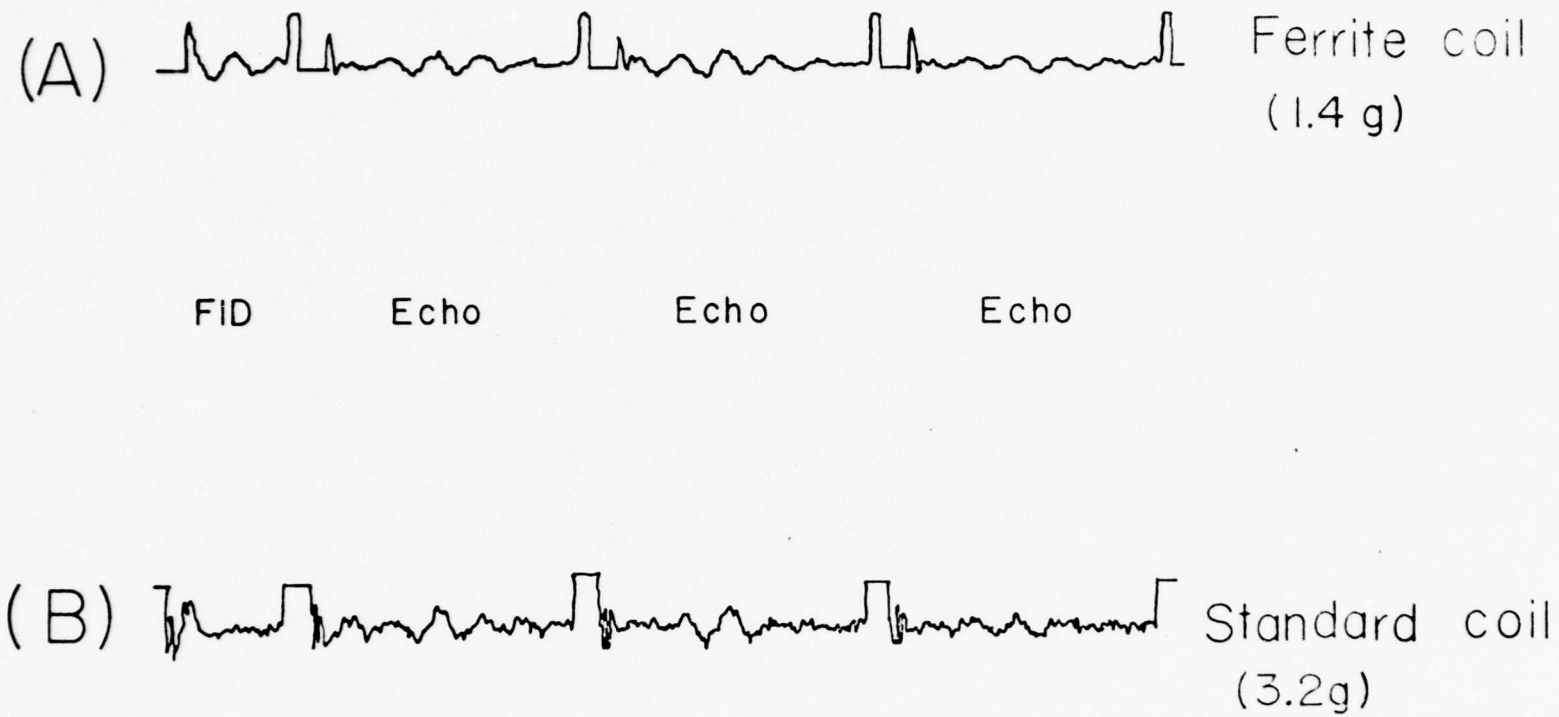

Figure 4.2.1-1 Comparison of NQR signal and noise obtained using a ferrite coil with signal from standard coil. Excitation sequence and signal processing was identical. The ferrite coil holds 1.4 grams of $NaNO_2$ in its gap, while the standard coil contains 3.2 grams of $NaNO_2$ mixed with a sugar filler in its 40 cc sample volume The data were normalized to the same peak amplitude by the signal processing and shows a better signal to noise for the ferrite coil.

This implies a remanent field of ≈10 gauss or so. Because of this finding, no attempt was made to study TNT by this technique, since it was estimated that its ηe^2qQ would be ≈400 KHz, and thus too small to overcome the remant field smearing.

c. Mechanical vibrations in the gapped toroids induced by the RF field of the pulses, have the effect of increasing the ring-down time to 3-4 msec for the smaller of the two toroids tried and to ~1 msec for the larger. These larger "dead times" make it impossible to take full advantage of the SLSE enhancement. It is possible that this effect could be reduced by choosing even more massive toroids, or by using different toroid geometry. Another possibility is to coat the toroids with a mechanically damping coating, such as is sometimes done to transformers.

5. NQR STUDY OF TNT

5.1 N^{14} NQR MEASUREMENTS

The primary aim of the current contract is to study the NQR characteristics of TNT and to attempt to use NQR techniques to elucidate the thorny problem of polymorphism in this substance[27,28,29]. Table 5.1-I is a summary of the Nitrogen-14 NQR spectrum of TNT, and Figure 5.1-1 depicts the chemical structure of a TNT molecule and its total NQR spectrum at 77°K. The line shape of a typical resonance line at 77°K is shown in Figure 5.1-2.

At liquid-nitrogen temperature (77°K) the NQR spectrum of TNT consists of twelve lines in the range 0.5 - 1.0 MHz. These twelve lines have been paired into six sets of ($\nu-$, $\nu+$) pairs corresponding to six inequivalent NO_2 groups in the solid state. Thus the quadrupole coupling constant*, e^2qQ, and the asymmetry parameter, η, can be unequivocally computed for each of the six sites. The pairings were made using a single N^{14}-H^1 double-resonance technique based on an observation by Smith and Cotts[30], and developed for CW spectroscopy by Marino and Oja[31]. In addition to identifying the six sites by their corresponding ($\nu-$,$\nu+$) pairs a further identification is made as shown in Figure 5.1.1. The six sites are divided into two groups of three sites each depending on their relative intensity. The appearance of three (3) sites with "strong" signals and three (3) sites with "weak" signals is interpreted as strong indication that two crystallographic phases are present, in unequal proportions.

---

* The quadrupole coupling constant, e^2qQ, measures the energy of interaction of the quadrupolar nucleus in an electric field gradient. The asymmetry parameter, η, is a dimensionless number which measures the departure from axial symmetry of the electric field gradient.

TABLE 5.1-I

NITROGEN-14 NUCLEAR QUADRUPOLE RESONANT FREQUENCIES FOR TNT

Temperature	Site #	$\nu-$ kHz	$\nu+$ kHz
77°K	1	801.8	895.4
	2	730.1	888.1
	3	767.3	875.6
	4	792.1	869.4
	5	729.7	861.8
	6	767.7	857.0
16°C	Unassigned	769	871.0
		752	860.4
		716	845.0
		743	843.8
		(714)*	838.0

* Tentative

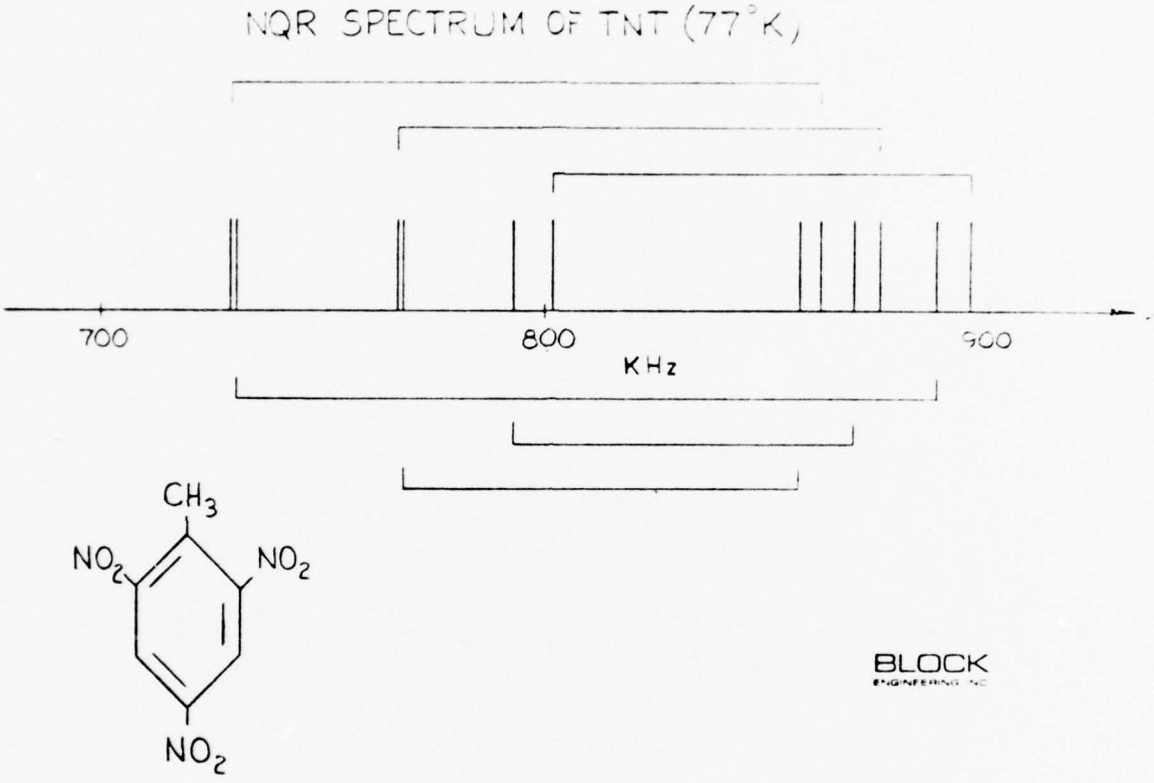

Figure 5.1-1 The Nitrogen-14 NQR spectrum of trinitrotoluene (TNT) at 77°K. Corresponding line pairs ($\nu-$,$\nu+$) are indicated. The lower diagram shows the chemical structure of TNT.

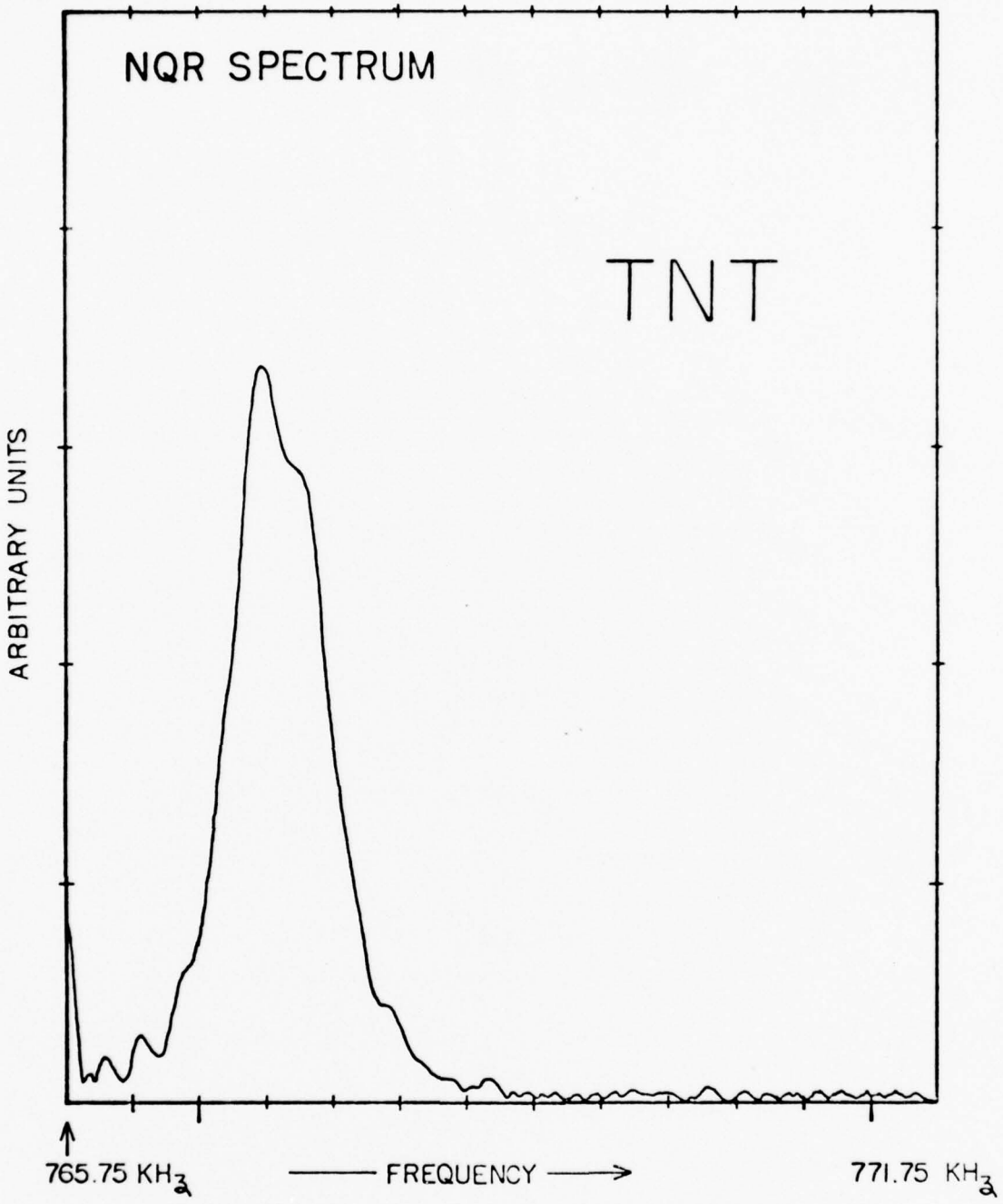

Figure 5.1-2 Line Shape of a typical NQR line of trinitrotoluene at 77°K.

With the aid of the drawing at the bottom of Figure 5.1.1 it is clear that each TNT molecule has two chemically distinct nitrogen sites, ortho and para to the methyl group. It is not unexpected that the chemical equivalence of the two ortho sites be broken in the solid state by the crystal field so that one would normally expect that each crystallographically distinct molecule give rise to three (3) distinct NQR sites. Then, the experimental observation of six (6) sites (twelve lines) is naturally interpreted as evidence for two physically distinct molecules. That these molecules belong to different phases instead of merely belonging to different crystallographic sites in the same phase is supported by the following observations.

a) The intensity of the two sites is different.

b) The relaxation times T_1 and T_2 are approximately the same for both sets of sites.

This combination of observations is most naturally explained by the presence of two crystal phases in unequal proportions. In Section 6 additional tests are suggested that can confirm these conclusions and are recommended for further study.

The observation of the room temperature spectrum of TNT is very difficult. The lines are weak to begin with because of the low resonant frequency, and their observation is made even more difficult by the unfavorable values of T_2 ($\approx$1 msec) encountered at ambient temperatures. With the aid of the SLSE technique (Section 3), however, it was possible to find 9 of the room temperature lines (out of the expected 12) with a 10th line listed as tentative. The "weak" ν-lines have been especially difficult to detect. It is expected that more work on this problem using the advanced techniques developed during this project will yield the remaining lines at room temperature. Until all twelve (12) room temperature lines are known, pairings of lines (ν+,ν-) cannot be properly made.

Finally, the results of a preliminary experiment where the frequency of TNT resonance lines were followed as a function of temperature between 77°K and room temperature are reported. During this research the lines become undectectable in the vicinity of 200°K. Then at cooler and warmer temperatures the lines were detected again, leading to the strong conjecture that the phase transition observed by Heberlein[32] can be studied and confirmed by NQR techniques. It is noted that in a more carefully controlled experiment the lines can be tracked closer to the transition point, and the nature of the transition (first or second order) can be learned from the shape of the frequency vs. temperature data. This is planned in future work.

6. RESULTS AND CONCLUSIONS

6.0 GENERAL

The present program has been an unqualified success. The objectives of the research have been met and the use of NQR spectroscopy as a means of characterizing explosives has been demonstrated. Furthermore, the data gleaned to date indicates a broad vista of research problems to which NQR can be applied in the field of explosives characterization and behavior and possibly quality control.

6.1 RESULTS

The principal area of research undertaken during this program was an effort to understand the crystalline structure of TNT. In particular it was desired that the behavior of TNT between 77°K and room temperature be studied. The results as indicated in Section 5 indicate that TNT has at least two (2) crystalline phases and an indication of at least one (1) phase transition at approximately 200°K. These results are based on locating twelve (12) TNT lines at 77°K and nine (9) lines at room temperature. The number of NQR lines observed are indicative of the crystalline phases while an abrupt change in frequency as a function of temperature for any one (1) line is indicative of a phase change.

The TNT results unto themselves are not a complete indication of the effort expended on this program. Room temperature TNT lines are too weak to be seen, with any degree of certainty, using standard pulsed NQR techniques. As a result of the necessity to measure these lines, a multiple pulse technique was developed under

the scope of this program. Using sodium nitrite ($NaNO_2$) as a reference,* it was determined that increased sensitivity factors between 10 and 100 are attainable. It is expected that by applying this approach, in future work, to the study of TNT, the three (3) missing room temperature lines of TNT can be found.

During the course of this program the practicality of measuring very small amounts of material using ferrite sample coils was also investigated. This work showed considerable promise but was not fully developed because it was not directly needed to obtain the TNT data necessary to meet the objectives of the program.

Five (5) technical publications are anticipated as a result of this work:

a. A communication on the initial announcement of the multiple pulse spin-locked spin-echo technique. (To appear in the Journal of Chemical Physics, 15 September 1977).

b. The detailed paper on the multiple pulse spin-locked spin-echo technique. (To be presented at the Fourth International Symposium on Nuclear Qaudrupole Resonance, Osaka, Japan and to be submitted to the Journal of Magnetic Resonance).

c. A detailed description of the pulsed NQR/FFT spectrometer. (To be presented at the Fourth International Symposium on Nuclear Quadrupole Resonance, Osaka, Japan and to be submitted to the Journal of Magnetic Resonance).

d. A report on the N^{14} NQR Study of TNT (Manuscript in preparation).

e. A discussion of ferrite coils for use with small samples (Manuscript in preparation).

* The NQR spectrum of $NaNO_2$ is well characterized and use of this compound permits a quantitative evaluation of the sensitivity gain attainable using the multiple pulse approach.

6.2 RECOMMENDATIONS

There are innumerable applications to which the NQR technique can be applied in the study of explosive characterization and behavior. These include:

a. A study of $N^{14}N^{15}$ TNT from 77°K to room temperature to aid in assigning the ortho and para sites.

b. A study of TNT from room temperature to 50°C to determine behavior patterns. (This wil require further modification to the extent NQR spectrometer so that the even weaker NQR lines at elevated temperature can be seen).

c. A study of Compound B which includes studying HNS/TNT and HMX/RDX mixtures.

d. A study of HMX and HMX complexes to determine why HMX will form chemical complexes while RDX (of related chemical structure) will not.

e. A study of the effect of shock waves on RDX samples to determine why some detonate and some do not. (Obviously only those that do not detonate can be researched).

f. A study of the thermal motion in azides to evaluate what factors contribute to their explosive value.

g. A further study of ferrite coils to determine whether they can be optimized for single crystal NQR spectroscopy of explosives.

h. A continuation of research work previously conducted by Block Engineering, Inc. on remote NQR (sample up to 12 inches from excitation and receiver coil) to evaluate this approach for shelf life studies, quality control, and booby trap detection.

The NQR technique, in the past, has been limited by poor instrumentation but with the unit presently available only at Block Engineering, explosives problems associated with chemical structure, crystallography and morphology can be properly researched.

REFERENCES

1. For the sake of simplicity we are defining one thermal relaxation time T_1. In reality in a three level system, such as N^{14} NQR, one expects and observes two thermal relaxation times sometimes called the short and long relaxation time T_{1s}, T_{1l}, respectively. This experimental and theoretical complication should not obscure the underlying physical meaning of these parameters.

2. A. Zussman and M. Oron, J. Chem. Phys. 66, 743 (1977).

3. S. Alexander and A. Tzalmona, Phys. Rev. 138, A845 (1965).

4. A. Zussman and S. Alexander, J. Chem. Phys. 49, 3792 (1968).

5. G. Petersen and T. Oja, Advances in Nuclear Quadrupole Resonance, Vol. 1, edited by J.A.S. Smith, (Heyden, London 1974) page 179.

6. Y. Abe, Y. Ohneda, M. Hirota, S. Kojima, J. Phys. Soc. Japan 37, 1061 (1974).

7. L. Guibé, Proceedings of the Second International Symposium on Nuclear Quadrupole Resonance Spectroscopy, edited by A. Colligiani (A. Vallerini, Pisa, 1975) page 95.

8. A Colligiani and R. Ambrosetti, Gazz. Chim, It. 106, 439 (1976)

9. A.A.V. Gibson, R. Goc, and T.A. Scott, J. Mag. Res. 24, 103 (1976).

10. S. Vega, J. Chem. Phys. 61, 1093 (1974).

11. H.Y. Carr and E.M. Purcell, Phys. Rev. 94, 630 (1954).

12. S. Mieboom and D. Gill, Rev. Sci. Instr. 29, 688 (1958).

13. R.A. Marino and S.M. Klainer, to be published 15 Sept., 1977, J. Chem. Phys.

14. E.D. Ostroff and J.S. Waugh, Phys. Rev. Letters 16, 1097 (1966).

15. P. Mansfield and D. Ware, Phys. Letters 22, 133 (1966).

16. A. Colligiani, R. Ambrosetti, and F. Salvetti, J. Chem. Phys. 60, 1871 (1974).

17. J. Koo, PhD. Thesis (1969) University of California, Berkeley.

18. D.T. Edmonds and P.A. Speight J. Mag. Res. 6, 265 (1972).

19. R. Blinc et al, J. Chem. Phys. 57, 5087 (1972).

20. J. Seliger et al, Phys. Stat. Sol. (a) 25,K121 (1974).

21. In the present case of polycrystalline NQR, we take a 90° pulse to be one that maximizes the free induction decay signal.

22. The shorter of the two relaxation times was much more difficult to measure since it appeared to depend critically on the magnitude of the excitation pulses. Both relaxation times, however, showed a similar dependence on τ.

23. G.L. Peters, PhD. Thesis, Brown University, 1975, Unpublished.

24. J.S. Waugh and C.H. Wang, Phys. Rev. 162, 209 (1967).

25. P. Mansfield and D. Ware, Phys. Rev. 168, 318 (1968).

26. M. Emshwiller, E.L. Hahn, and D. Kaplan, Phys. Rev. 118, 414 (1960).

27. L.A. Burkhardt and D.H. Bryden, Acta Cryst., 7, 135 (1954).

28. Grabar, Rauch and Fanelli, J. Phys. Chem. 73, 3514 (1969).

29. Chick, Connick and Thorpe, Journal of Crystal Growth 7, 317 (1970).

30. D.H. Smith and R.M. Cotts, J. Chem. Phys. 41, 2403 (1964).

31. R.A. Marino and Tonis Oja, J. Chem. Phys. 56, 5433 (1972).

32. D.C. Heberlein, J. Chem. Phys. 61, 2346 (1974).

APPENDIX A
NQR THEORY

A. NUCLEAR QUADRUPOLE RESONANCE (NQR) THEORY

A.1 INTRODUCTION

The technique of NQR developed as an outgrowth of the discovery of NMR in the late forties. The theory of nuclear quadrupole interaction in solids was first given by R. V. Pound at Harvard in 1950, and later that year Dehmelt and Kruger in Germany observed the NQR signal from the chlorine-35 (Cl^{35}) nucleus in transdichloroethylene. In the following year Watkins and Pound detected the first quadrupole resonance from nitrogen-14 (N^{14}) in HMT (hexamethylenetetramine), BrCN and ICN. Experimental difficulties delayed the utilization of the NQR and until the late sixties only a few compounds were studied. Two chief difficulties arise in N^{14}:

(1) the low frequency range of the resonance lines (0.5 to 5 MHz) which makes them weak and hard to detect, and

(2) The unusually strong intermolecular interactions which are characteristic in nitrogen-containing compounds preclude on one hand the proper transfer of radio-frequency energy to the crystalline lattice, and on the other hand make the electric field gradient very sensitive to the purity and crystallinity of the material.

This results in transitions which are easily saturated and lines which are too broad to be detected with conventional (cw) spectrometers. With the development of pulsed methods and more sensitive spectrometers these difficulties can be overcome. At the present time N^{14} NQR is successfully being applied using the Block Engineering, Inc. NQR/FFT Spectrometer.

A.2 BASIC CONCEPTS OF NQR

In order to understand the origin of nuclear quadrupole resonance, we may visualize a nucleus as a classical distribution of positive charges, $\rho_N(\vec{r})$, over a volume of characteristic linear dimensions of the order of nuclear radii: 10^{-13} cm (Figure A-1). A charge cloud extending over a volume of linear dimensions of the order of several angstroms generates an electrostatic potential $\phi(\vec{r})$ which can be considered as varying slowly over the region occupied by the nucleus. The electro-static energy of the system expressed as

$$W = -\int \rho_N(\vec{r})\,\phi(\vec{r})\,d\vec{r} \qquad \text{(A-1)}$$

can then be expanded in terms of the moments of the nuclear charge distribution:

$$W = -\phi(0)q_N + \vec{p}\cdot\vec{E}(0) - \frac{1}{6}\sum_{ij} q_{ij}Q_{ij} + \ldots \qquad \text{(A-2)}$$

where

q_N	$= \int \rho_N(\vec{r})\,d\vec{r}$	nuclear charge
$\vec{p}$	$= \int \rho_N(\vec{r})\,\vec{r}\,d\vec{r}$	dipole moment vector
Q_{ij}	$= \int \rho_N(\vec{r})\,x_i x_j\,d\vec{r}$	quadrupole moment tensor
$\vec{E}$	$= -\vec{\nabla}\phi$	electric field vector
q_{ij}	$= \partial E_i/\partial x_j$	electric field gradient tensor

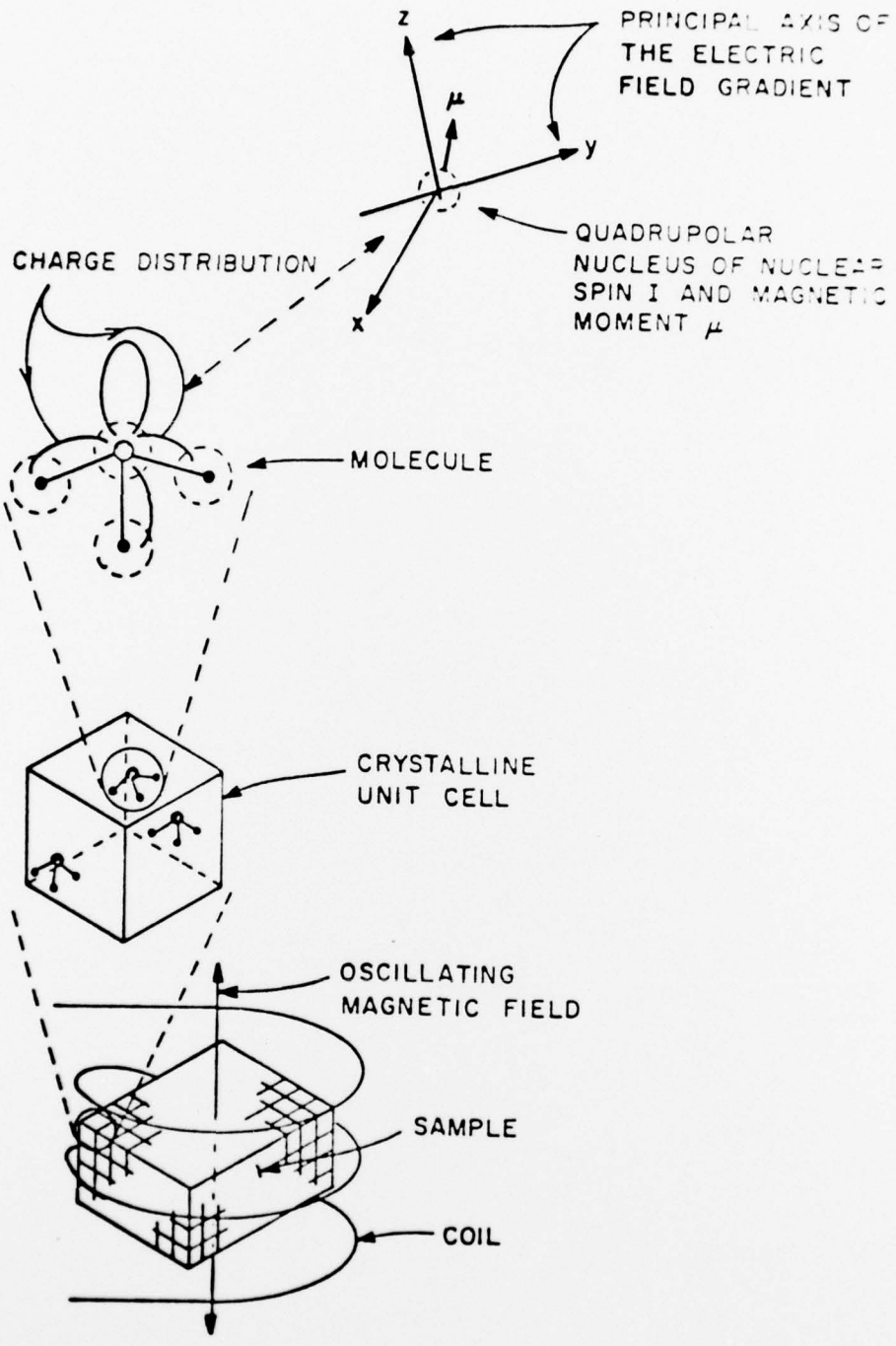
z
PRINCIPAL AXIS OF
THE ELECTRIC
FIELD GRADIENT
μ
y
QUADRUPOLAR
NUCLEUS OF NUCLEAR
SPIN I AND MAGNETIC
MOMENT μ
x
CHARGE DISTRIBUTION
MOLECULE
CRYSTALLINE
UNIT CELL
OSCILLATING
MAGNETIC FIELD
SAMPLE
COIL

Figure A-1

From quantum mechanical considerations it can be proven that the only non-vanishing terms in (2) are the first and third ones. Then, if the energy of the system is referred to the constant first term:

$$W_Q = -\left[W + V(0)q_N\right] = \frac{1}{6}\sum_{ij} q_{ij}Q_{ij} \qquad \text{(A-3)}$$

Q_{ij} is diagonal and is related to the components of the nuclear spin I_i according to

$$Q_{ij} = \frac{eQ}{I(2I-1)}\left[3I_i^2 - I(I+1)\right] \qquad \text{(A-4)}$$

where $I = \left(\sum I_i^2\right)^{\frac{1}{2}}$ and eQ is defined as the nuclear quadrupole moment. Since

$$\sum_i q_{ij} = 0 \quad \text{(Laplace equation: } \Delta\phi = 0\text{)}$$

the quantum mechanical expression of the quadrupole energy (the Hamiltonian) takes the particular simple form:

$$H_Q = \frac{eQ}{2I(2I-1)}\sum_i q_{ij}I_i^2 \qquad \text{(A-5)}$$

which can also be expressed in the following way:

$$H_Q = \frac{e^2qQ}{4I(2I-1)}\left[(3I_z^2 - I^2) + \eta(I_x^2 - I_y^2)\right] \qquad \text{(A-6)}$$

where e^2qQ is defined as the quadrupole coupling constant of the system and η is defined as the asymmetry parameter of the electric field gradient (efg):

$$\eta = \frac{q_{xx} - q_{yy}}{q_{zz}} \qquad \text{(A-7)}$$

$$e^2qQ = (eQ)(eq_{zz})$$

where

$|q_{zz}| > |q_{yy}| > |q_{xx}|$ by convention.

For nitrogen-14, of nuclear spin I = 1, the solution of the Schroedinger equation $H_Q \psi_N = E \psi_N$, where ψ_N is the nuclear wave function, can be shown to lead to a three level system of energies given by

$$E_z = e^2qQ/2$$

$$E_x = -E_z(1-\eta)/2 \qquad \text{(A-8)}$$

$$E_y = -E_z(1+\eta)/2$$

Transitions between these levels can be induced with oscillating magnetic fields of the proper (resonant) frequencies. The frequencies of these transitions

$$\nu_+ = \frac{e^2qQ}{4h}(3+\eta)$$

$$\nu_- = \frac{e^2qQ}{4h}(3-\eta) \qquad \text{(A-9)}$$

$$\nu_d = \frac{e^2qQ\eta}{2h} = \nu_+ - \nu_-$$

Conversely, determining any two of the three NQR frequencies completely describes the efg in the vicinity of the nitrogen nucleus:

$$e^2qQ = \frac{2}{3}(\nu_+ + \nu_-)$$

$$\eta = \frac{2(\nu_+ - \nu_-)}{e^2qQ} \qquad \text{(A-10)}$$

Experimental techniques for the determination of NQR spectra can be divided into three categories:

(a) Continuous-wave (cw) methods
(b) Transient methods
(c) Double resonance techniques.

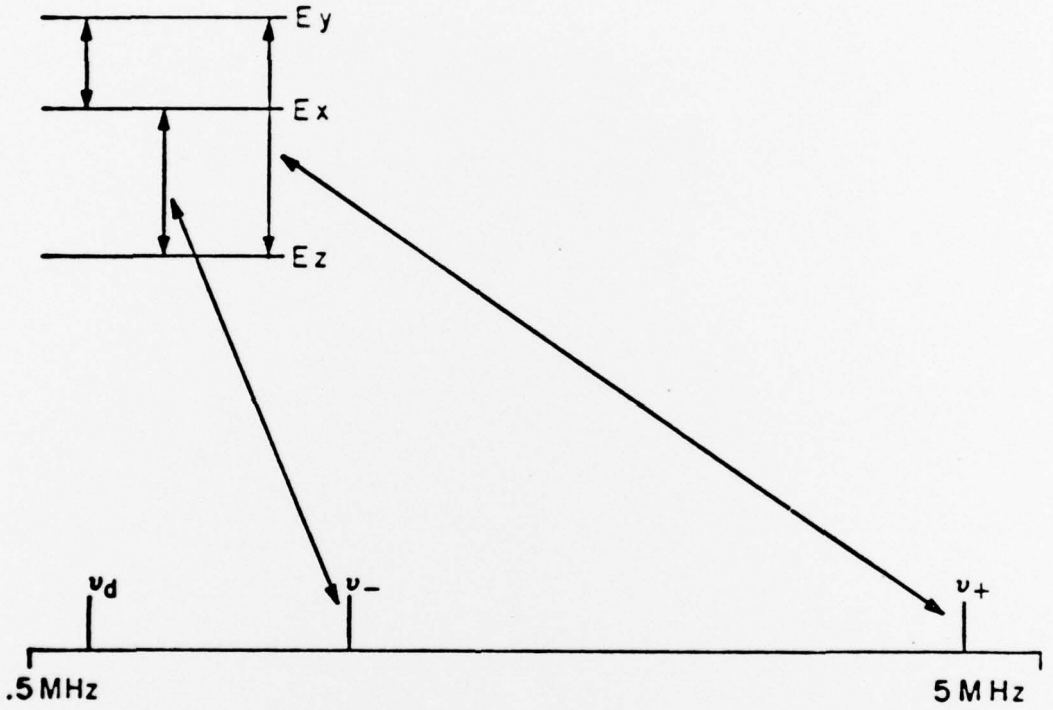

Figure A-2

CW methods have enjoyed great popularity for they are simple and inexpensive. The limitations of these techniques are so severe, however, that at least in the Nitrogen-14 NQR field they are rarely used any more. Transient methods include the superregenerative technique, which for Nitrogen-14 is bad and rarely used, and pulsed methods. Double resonance techniques are essentially pulsed methods that monitor the resonance of one type of nuclear species while another is being perturbed. Even though they are extremely sensitive they are very complicated and have not yet enjoyed the popularity of regular pulsed methods.

The Nitrogen-14 pulsed techniques that operate in the so-called spin-echo mode are particularly good (for other nuclei the reverse holds true, and cw or superregenerative methods are better).

To understand the reasons for this advantage let us begin by defining some basic magnitudes that describe an NQR line. In the frequency domain an NQR line is fully described by its frequency and by a normalized shape function S(w). For example:

$$S(w) = \frac{2}{\pi_{\Delta w}} \frac{1}{1 + \left(\frac{w-wo}{\Delta w}\right)^2} \qquad \text{(A-11)}$$

Spin-echo techniques operate in the time domain, there are three parameters that fully describe an NQR absorption line

(a) Spin-lattice relaxation time (T_1). The typical "waiting" time to observe a resonance a second time.

(b) Spin-spin relaxation time. (T_2). A magnitude which establishes the time scale for the observation of spin-echoes.

(c) A spin-echo shape function G(t). The "width" of this function is defined as $2T_2^*$. G(t) is the fourier transform of the line shape function S(w), thus $T_2^* = \frac{1}{\Delta w}$.

CW and superregenerative methods are poor techniques for Nitrogen-14 because of the generally large T_1 and large Δw values associated with an NQR line (to avoid saturation in cw the level has to be reduced to very small values). Broad lines, a very common occurrence with Nitrogen-14, are weak since their areas are constant. Spin-echo methods are, on the other hand, unaffected by long T_1 values and since G(t) and S(w) are related by a fourier transformation the equality

$$G_{MAX} = \int_0^\infty S(w)\, dw = 1 \qquad \text{A-12}$$

holds (Figure A-3). Thus broad lines in the frequency domain do not affect the maximum intensity of the echo signal. In addition, pulsed methods for Nitrogen-14 are particularly advantageous because T_2 times are generally long (of the order of milliseconds). This is a result of the "spin quenching" effect for $\eta \neq 0$ which substantially reduces spin-spin interactions.

The Nitrogen-14 NQR spectrum of a molecular system is determined by placing about 25 grams of sample inside the inductor of a tank circuit which is then subjected to a series of radiofrequency pulses of frequency f. Whenever the frequency of these pulses satisfies the resonance condition $f = \nu_Q$ where ν_Q is one of the quadrupole frequencies - absorption of energy takes place and is retransmitted as a series of signals (FID or free induction decay and spin echos) as is shown schematically in Figure A-4.

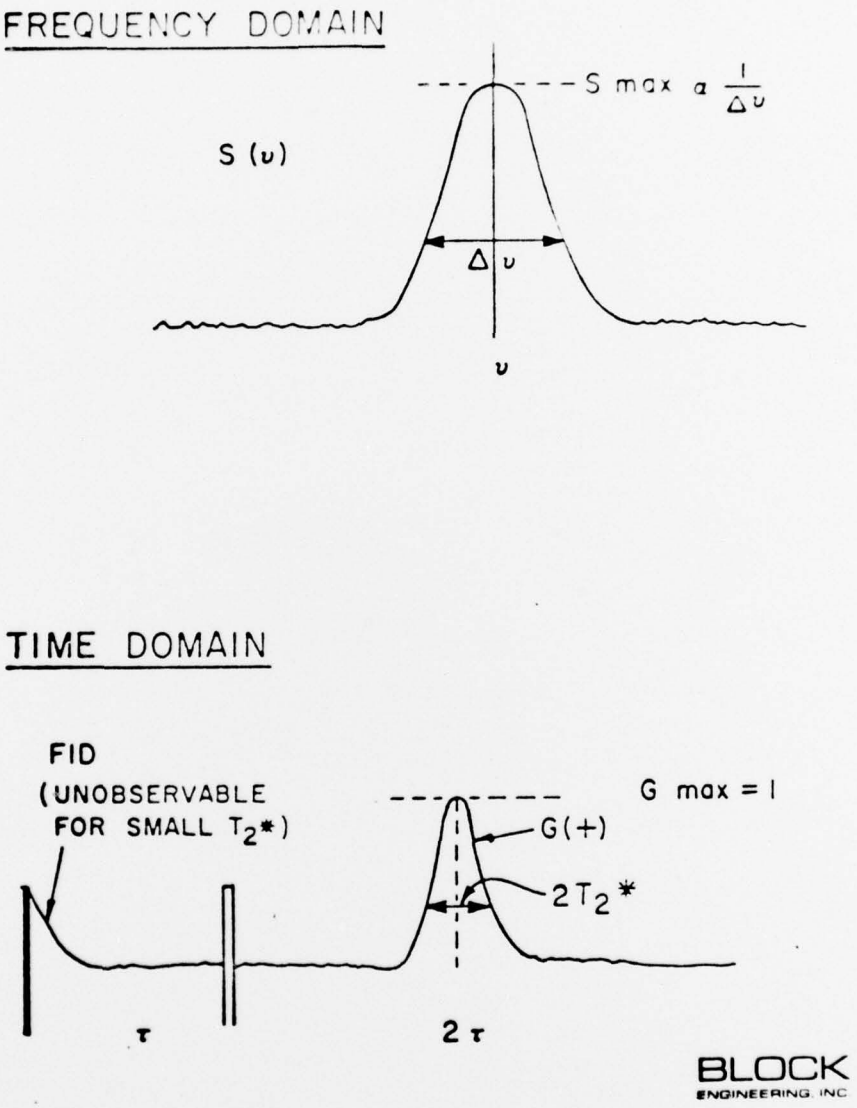
FREQUENCY DOMAIN
S max α 1/Δυ
S (υ)
Δ υ
υ
TIME DOMAIN
FID
(UNOBSERVABLE
FOR SMALL T2*)
G max = 1
G(+)
2T2*
τ
2τ
BLOCK
ENGINEERING, INC

Figure A-3

Therefore, by monitoring and detecting the transmitted signals as a function of the frequency of the pulses, the energy levels of the quadrupole nucleus are completely determined.

Since a narrow rf pulse has a fourier spectrum of finite width, the pulse frequencies can be varied in discrete steps (5-10 kHz) so as to cover a larger frequency range for a given observation time. In this manner the total frequency range is only limited by the "waiting period" between successive observations. This waiting period depends on the spin lattice ralxation time (T_1) of the particular compound which is being investigated. This can be quite long (5 - 10 min.) for Nitrogen-14 NQR.

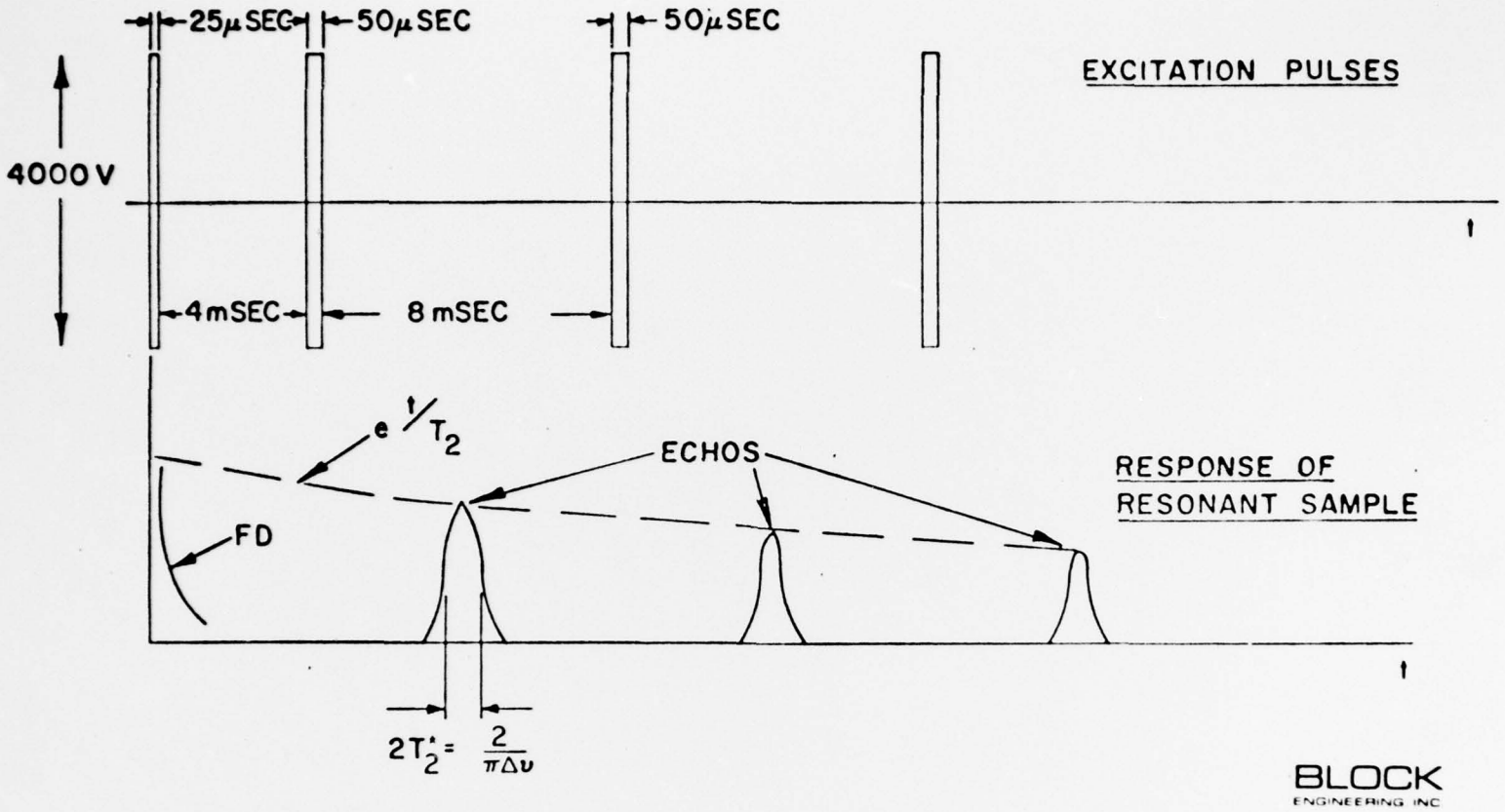
25μSEC
50μSEC
50μSEC
EXCITATION PULSES
4000 V
t
4mSEC
8 mSEC
e
1/T2
ECHOS
RESPONSE OF
RESONANT SAMPLE
FD
t
2T2* = 2/πΔυ
BLOCK
ENGINEERING INC

Figure A-4